ICG
International Centre for Geohazards

ICG project 2

Vulnerability and Risk Assessment for Geohazards

Case studies: Risk associated with avalanches

ICG Report 2006-2-2

NGI Report 20061032-02 30 November 2007

Partners in ICG

NGI

UNIVERSITAS OSLOENSIS MDCCCXI

NTNU

NGU Norges geologiske undersøkelse

NORSAR

Client: **The Research Council of Norway**

Contact person:

Contract reference:

For

Project Manager: Suzanne Lacasse

Report prepared by: Peter Gauer

Reviewed by: Suzanne Lacasse

Postal address: P.O. Box 3930 Ullevaal Stadion, N-0806 OSLO, NORWAY
Street address: Sognsveien 72, OSLO
Internet: http://www.geohazards.no
Telephone: (+47) 22 02 30 00
Telefax: (+47) 22 23 04 48
e -mail: icg@ngi.no
Postal account: 0814 51 60643
Bank account: 5096 05 01281
Business No. 958 254 318 MVA

Summary

This report documents an approach for the probabilistic risk assessment for avalanches. It presents two case studies:

1) A case regarding the risk to a building in an avalanche path;
2) A study concerning the risk to traffic on a major mountain road.

Estimates of hazard, vulnerability and risk are given. The methodology adopted in the present case study refers to the general risk terminology from ICG (2004).

The report summarizes vulnerability values due to avalanche impacts retrieved from the literature.

In the first case study of a farm in an avalanche path, a combination of empirical meteorological data (extreme snow precipitation data), a slide release model, and a runout model employing Monte-Carlo simulations in both cases are used to quantify hazard and risk.

The second case study considers traffic along a road stretch in avalanche-prone area and reveals high risk to individuals. A comparison between the risk with and without a mitigation measure (i.e. with and without a protection gallery) shows the beneficial effect of the mitigation measure. However, waiting traffic increase significantly the risk, which implies that after an avalanche event immediate action is needed to avoid waiting traffic.

The case studies illustrate the methods, but do not claim to be generally valid. A main challenge for the proposed methods is the choice of realistic distribution functions and their parameters. Not enough knowledge is available on this subject. To fill those gaps, expert judgment needs to be applied, more data should be gathered, and more research should be carried out. Deterministic models support the probabilistic approach for the choice of parameters.

Contents

1 INTRODUCTION

This report documents an approach for the probabilistic assessment of risk associated with snow avalanches.

Avalanches constitute a considerable natural hazard in snow-covered mountain areas. They are fast moving masses of snow and debris on (steep) mountain slopes, which can cause catastrophic destruction. During precipitation and/or storm periods, snow accumulates on slopes. Blowing and drifting snow is in many cases responsible for intense loading of slopes. As long as the shear strength within the snowpack is larger than the component of its weight parallel to the slope, the snowpack will be stationary. Subsequently, at some critical snow depth, the shear resistance will be overcome and a slide will be released. In addition, external loads can contribute to the release of a slab, like a skier or loading by explosives as done for temporal mitigation. Also the reduction of the strength, for example due to rapid warming (e.g. during foehn) or rain, can cause an avalanche release. During their descent, avalanches may reach velocity up to 100 m s^{-1}; the flowing density is thought to range typically between 30 to 300 kg m^{-3}. Thus, impact pressures can be as high as several hundred kPa.

The report presents methods to quantify avalanche hazard and risk in a probabilistic framework. A combination of empirical meteorological data (extreme snow precipitation data) and a simple slide release and a topographical runout model (in both cases using Monte-Carlo simulations) is employed. Two case studies are presented: 1) a case regarding the risk to a building in an avalanche path; 2) a study concerning the risk to traffic on a major mountain road. Estimates of hazard, vulnerability and risk are given.

In the first part of the report, a brief literature review summarizes present approaches and knowledge concerning hazard, vulnerability, and risk with respect to avalanches from the perspective of a generalized integrated risk assessment framework.

2 GENERALIZED INTEGRATED RISK ASSESSMENT FRAMEWORK

Effective assessment of risk associated with geohazards hazard requires a systematic approach. In engineering, the final result of any risk assessment should be a quantitative description of the risk, which can be communicated and can form the basis for decision-making. This so-called quantitative risk assessment (QRA) intends to find answers to following questions (Ho *et al.* 2000, Lee and Jones 2004):

1 **Danger Identification:** What are the probable dangers/problems?

2 **Hazard Assessment:** What would be the magnitude of dangers/problems?

3 **Consequence/Elements at Risk Identification:** What are the possible consequences and/or elements at risk?

4 **Vulnerability Assessment:** What might be the degree of damage in elements at risk?

5 **Risk Quantification/Estimation:** What is the probability of damage?

6 **Risk Evaluation:** What is the significance of estimated risk?

7 **Risk Management:** What should be done?

2.1 Terminology

To communicate risk and related issues, it is important to use a common terminology. The proposed terminology for risk assessment at NGI and ICG (ICG, 2004), is:

- **Consequence:** In relation to risk analysis, the outcome or result of a hazard being realized.
- **Danger (Threat):** The natural phenomenon that could lead to damage, described in terms of its geometry, mechanical and other characteristics. The danger can be an existing one (such as a creeping slope) or a potential one (such as a rock fall). The characterization of a danger or threat does not include any forecasting.
- **Elements at risk**: Population, buildings and engineering works, infrastructure, environmental features and economic activities in the area affected by a hazard.
- **Hazard:** Probability that a particular danger (threat) occurs within a given period of time.
- **Probability:** A measure of the degree of certainty. This measure has a value between zero (impossibility) and 1.0 (certainty). It is an estimate of the likelihood of the magnitude of the uncertain quantity, or the likelihood of the occurrence of the uncertain future event.
- **Risk:** Measure of the probability and severity of an adverse effect to life, health, property, or the environment. Quantitatively,

  $$\textbf{Risk} = \textbf{Hazard} \times \textbf{Potential Worth of Loss} \qquad (2.1)$$

  This can be also expressed as "Probability of an adverse event times the consequences if the event occurs". Various formulations for risk can be found in (Düzgün and Lacasse, 2005).
- **Risk assessment:** The process of making a decision recommendation on whether existing risks are tolerable and present risk control measures are adequate, and if not, whether alternative risk control measures are justified or will be implemented. Risk assessment incorporates the risk analysis and risk evaluation phases.
- **Risk evaluation**: The stage at which values and judgment enter the decision process, explicitly or implicitly, by including consideration of the importance of the estimated risks and the associated social, environmental,

and economic consequences, in order to identify a range of alternatives for managing the risks.

- **Risk management:** The systematic application of management policies, procedures and practices to the tasks of identifying, analysing, assessing, mitigating and monitoring risk.
- **Vulnerability:** The degree of loss to a given element or set of elements within the area affected by a hazard. It is expressed on a scale of 0 (no loss) to 1 (total loss).

2.2 Avalanche hazard

Several factors contribute to avalanche hazard including terrain, weather, and niveological conditions.

2.2.1 Terrain

Snow covered slopes need to have certain steepness otherwise the snow will not slide. Typically, catastrophic avalanche originate from slope between 30 and 35°. Steeper slopes tend to avalanche more frequently and so the snow accumulation is less. In few occasions, avalanches start on slopes less than 30°; this is more common during wet snow conditions.

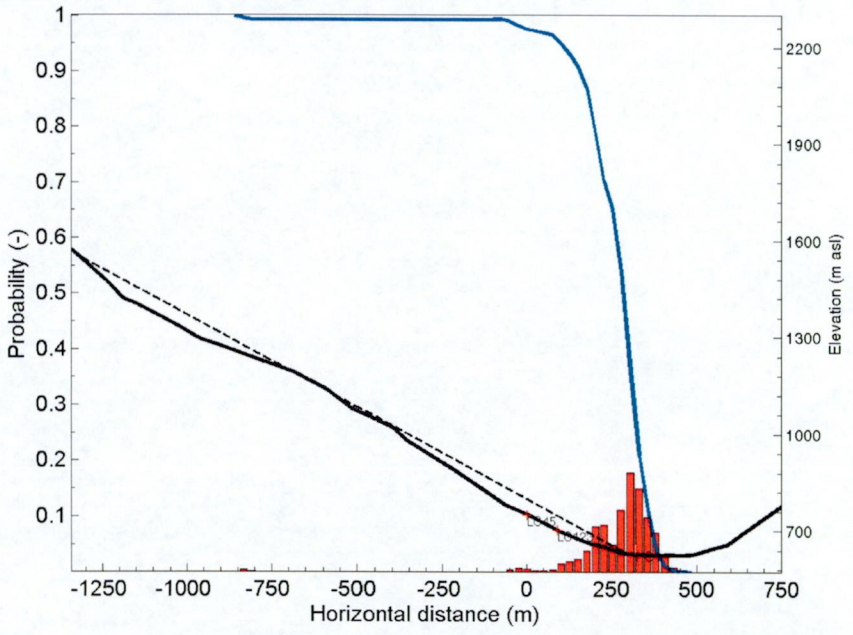

Figure 2.1 Probability of reaching a point along the avalanche; Monte-Carlo simulation with the runout ratio as random variable. Blue line shows the cumulative probability, P_{travel}, and the red bars the probability mass distribution. The example shows the track of the avalanche test-site Ryggfonn. The horizontal origin is set to the location of sensor mast LC45.

The profile of a track influences the probability that a specific location along the track is reached by an avalanche. This is the basis for statistical runout models like the α-β model (Bakkehoi *et al.* 1983), or those based on the energy line method or runout ratio (Körner, 1980). The runout ratio is defined as the ratio between vertical drop height and horizontal travel distance and is a measure for the efficiency of a slide to transform potential energy into translation. Barbolini and Savi (2001) used Monte-Carlo approach combined with deterministic avalanche model to calculate runout distances. Figure 2.1 shows an example of the probability of an avalanche reaching a point at a horizontal distance along the track. The calculations are based on Monte-Carlo simulation using an energy line approach. The choice of parameter distribution however, suffers from a lack of knowledge with respect to a possible volume dependence of the runout length. In addition, the influence of the snow properties in the track is uncertain.

2.2.2 Meteorology conditions

Meteorology conditions favouring avalanches are intense snowfall with strong winds. It is widely accepted that one of the most important meteorological parameters relevant for the release of catastrophic avalanches is the 3-day precipitation accumulation, HNW(3d) (Bakkehoi, 1987; McClung and Schaerer, 2006). HNW(3d) is the water equivalent of the 3 day snowfall. Figure 2.2 shows an example of the three-day precipitation, HMW(3d), versus return period, T_r. The probability of occurrence is approximated by $1/T_r$.

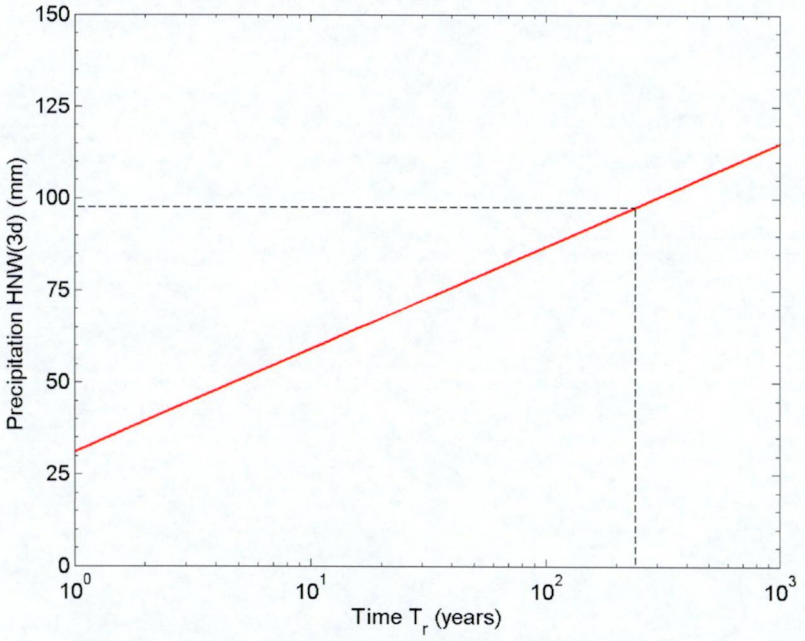

Figure 2.2 Three-day snow precipitation sum versus return period T_r. (Dashed lines indicate the example value.)

2.2.3 Niveological conditions

Niveological conditions favouring avalanche release are pre-existing weak layers, like depth hoar or cover surface hoar, which are than excessively loaded by, e.g. new snow, drifting snow, or explosives as done for temporal mitigation. Depending on the strength, a certain amount of loading is required to release a slide. Observations indicate that the probability of slide release correlates well with the three-day precipitation for a given avalanche path as it is show in Figure 2.3 for the case of five avalanche path.

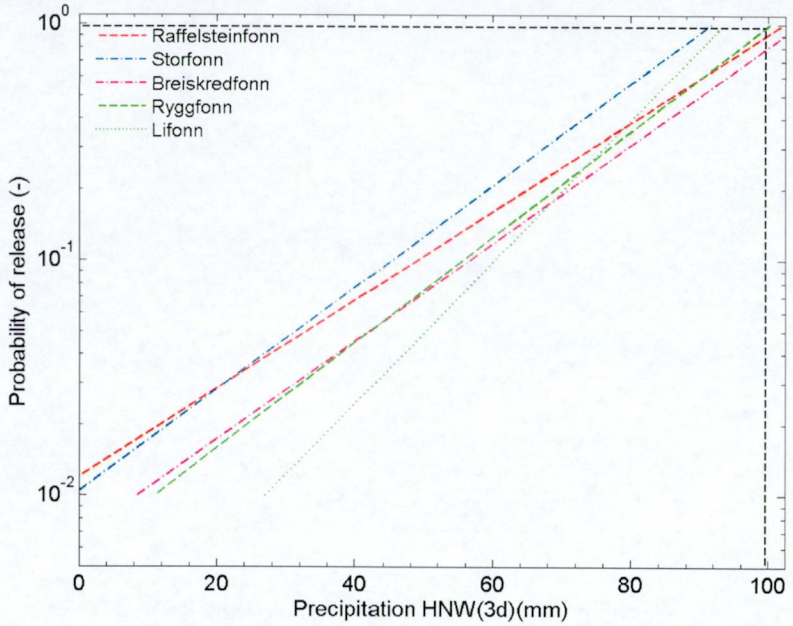

Figure 2.3 Cumulative probability of slab release for five three-day precipitation, HNW(3d), records (Bakkehoi, 1987). (Dashed lines indicate the example value.)

The hazard at a certain location along an avalanche track may be expressed as the product of the probability, P_{slide}, that a slide is released times the probability, P_{travel}, that the slide actually reaches the point. The former probability can be estimated by the integral of the conditional probability of slide release assuming an additional loading due to precipitation times the probability that the amount of precipitation occurs over all possible precipitation accumulations:

$$P_{slide} = \int_0^{\infty} P_r(\text{Release} \mid HNW < HNW_0) \bullet P_r(HNW = HNW_0)\ \mathrm{d}\,HNW \cdot \qquad (2.2)$$

Figure 2.4 shows the calculated probability, P_{slide}, taking the return period of the three-day precipitation from Figure 2.2 and the release probability for the Ryggfonn example in Figure 2.3. Taking a precipitation of 97.5 mm, the return period for such an event is 241 years or a probability of 4.2 $1 \cdot 0^{-3}$ per year, and

the release probability is 0.87. The cumulative probability that a slide can be observed for a 97.5 mm precipitation event is 6.3 $1 \cdot 0^{-3}$, whereas product of the single probabilities is only 3.7 $1 \cdot 0^{-3}$, which would underestimate the hazard.

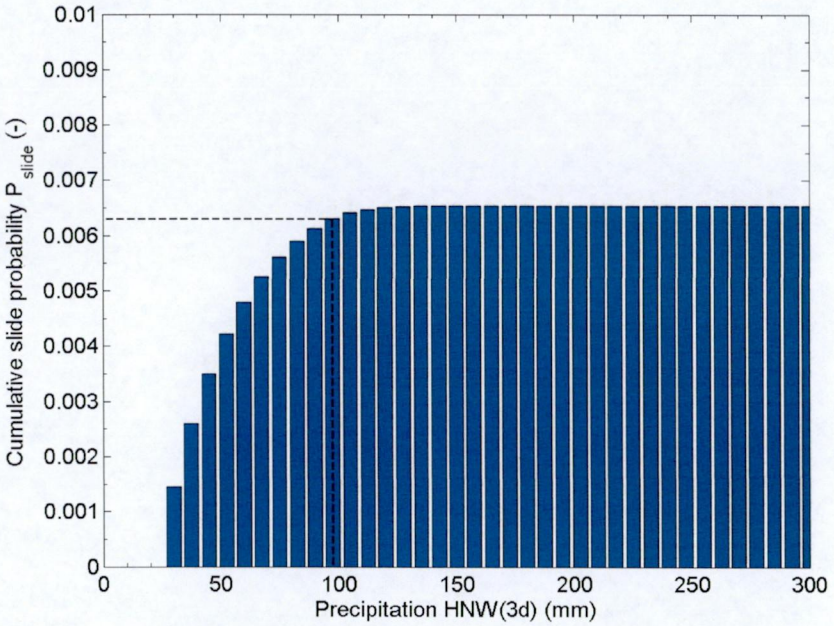

Figure 2.4 Cumulative probability of slide occurrence versus precipitation. (Dashed lines indicate the example value.)

The avalanche hazard, H, at a specific location is then given by the probability, P_{slide}, of a slide occurrence times the probability, P_{travel}, that the slide actually reaches the point of concern:

$$H = P_{slide} \bullet P_{travel} \cdot \tag{2.3}$$

2.3 Vulnerability

Besides the actual hazard, the vulnerability of an endangered object contributes to the risk. In recent years, several studies considered the vulnerability of humans and objects exposed to avalanches. There is, however, a considerable scatter in the proposed values. In the following, an overview of proposed vulnerability curves and values are presented. In addition to those proposals, which are based on avalanche observations, a comparison is given to observations on the vulnerability of buildings originating from nuclear tests. To define the vulnerability of an object, it is necessary to relate the vulnerability to an intensity measure. In the case of avalanches, an obvious intensity measure is the impact pressure of the slide, even though it is not always easy to determine as avalanche speed and flow density not always know for certain.

In the following, a summary of proposed specific loss and vulnerability values are reported for

- Buildings
- Persons in buildings
- Persons in cars
- Persons outdoors

2.3.1 Buildings

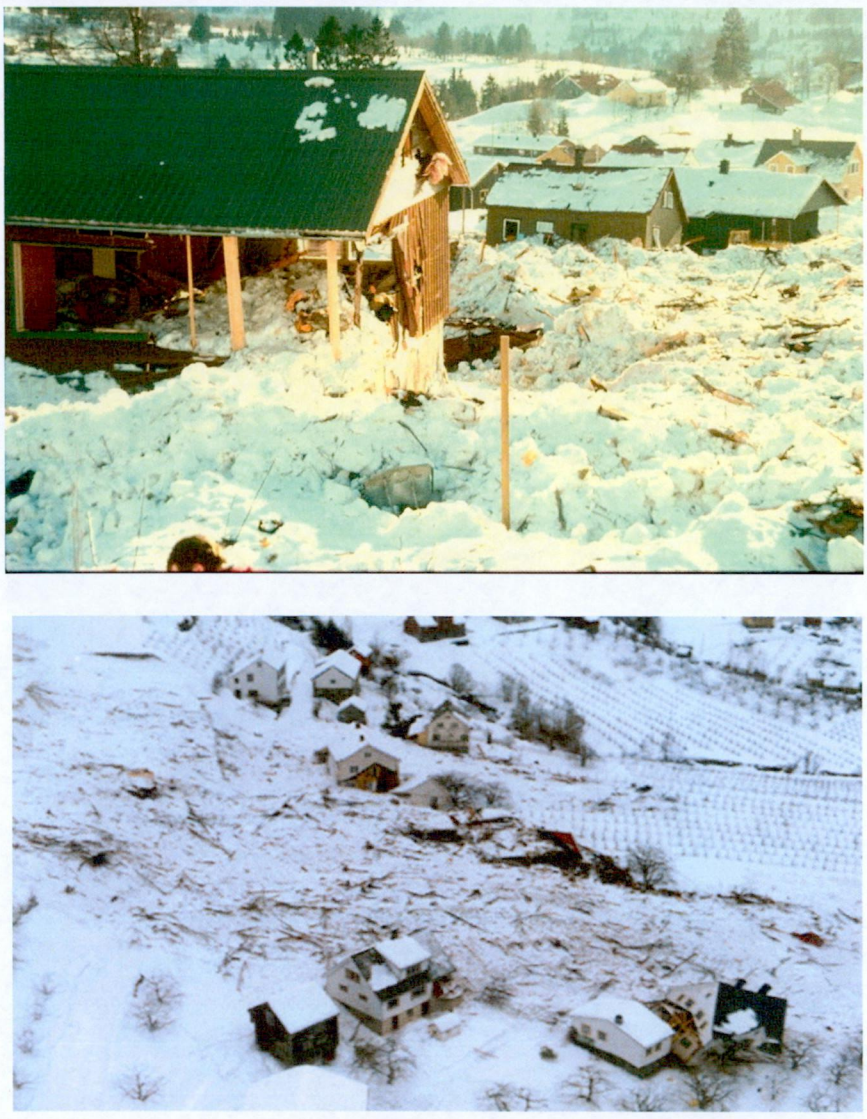

Figure 2.5 Vulnerability of houses to avalanche impacts (photo NGI).

Vulnerability for buildings is often presented as function of the "specific-loss" versus the "Impact pressure". With "specific loss", the authors mean the degree of damage and in ranges between zero and one, where zero is no damage and one stands for total destruction.

2.3.1.1 Wilhelm (1997)

Wilhelm (1997) relates the specific-loss to a building directly to the impact pressure (see Figure 2.6). The loss curves are developed based on observed destruction and back-calculation of the impact pressures to cause the destruction.

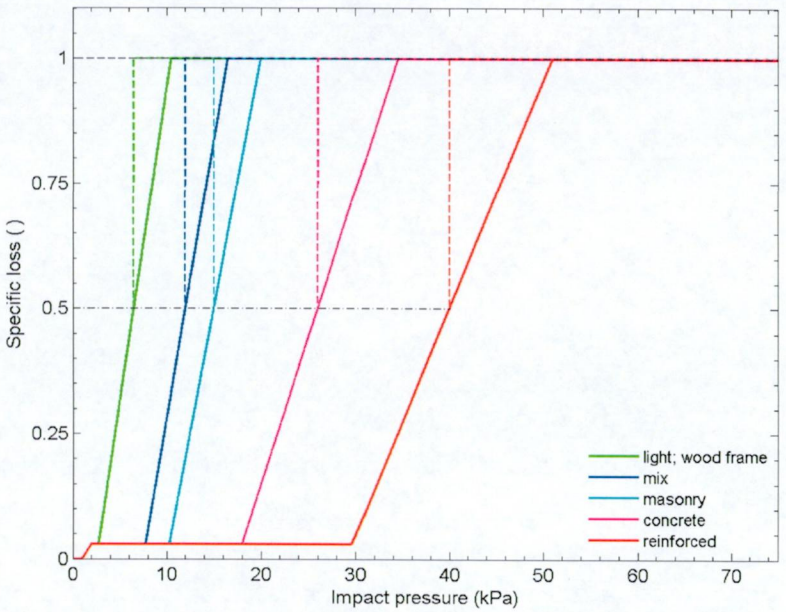

Figure 2.6 Specific loss versus impact pressure (Wilhelm, 1997). The dashed line indicates the serviceability of the building; that means after reaching a certainty specific loss it is no longer worth or possible to repair the building.

2.3.1.2 Keylock *et al.* (1999)

Keylock *et al.* (1999) relate the specific loss, SL, to the degree of damage, DD, by the equation

$$SL = \frac{4DD^2}{100}. \tag{2.4}$$

The corresponding values of DD are defined based on observed destruction (Table 2.1). In a second step, the DD values might be related to the Canadian avalanche size classification (CASC; Appendix A) and so to an impact pressure (Table 2.2). Compared to the specific losses given by Wilhelm (1997), the values are rather low for comparable impact pressures.

Table 2.1 Degree of damage to buildings (Keylock et al., 1999)

Degree of damage	DD	Phenomena observed
None	1	No visible damage to structural elements; possible fine cracks in wall and ceiling mortar; barely visible non-structural and structural damage.
Slight	2	Cracks in wall and ceiling mortar; falling of large patches of mortar from wall and ceiling surface; considerable cracks in or partial failure of chimneys, attics and gable walls; disturbance, partial sliding, sliding and collapse of roof covering; cracks in structural members.
Moderate	3	Diagonal or other cracks in structural walls, walls between windows and similar structural elements; large cracks in reinforced-concrete structural members (columns, beams, reinforced-concrete walls); partially failed or failed chimneys, attics, gable, walls disturbance, sliding and collapse of covering.
Heavy	4	Large cracks with or without detachment of walls, with crushed wall material between windows and similar elements of structural walls; large cracks with slight dislocation of reinforced-concrete structural elements (columns, beams and reinforced-concrete walls); slight dislocation of structural elements and the whole building.
Severe	5	Structural members and their connections undergo extreme damage and dislocation; many crushed structural elements; substantial dislocation of the entire building and damage to roof structure; partial or complete failure.

Table 2.2 Specific loss for two different construction types (Keylock et al., 1999)

CASC	Impact pressure (kPa)	Low-quality construction; wooden frame	Reinforced-concrete Structures
1	1	0	0
1.5	3	0	0
2	10	0.07	0.04
2.5	30	0.12	0.07
3	100	0.20	0.12
3.5	220	0.30	0.18
4	500	0.39	0.24
4.5	700	0.66	0.40
5	1000	0.82	0.50

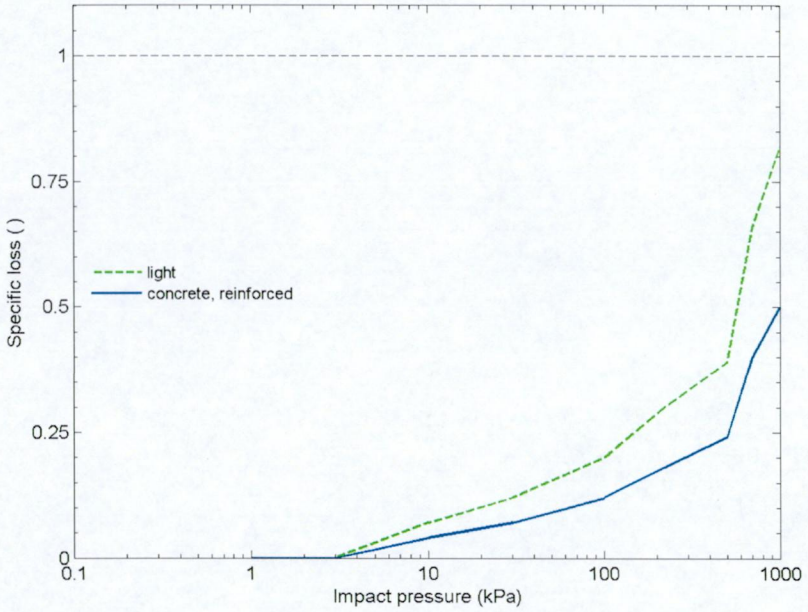

Figure 2.7 Specific loss versus impact pressure (after Keylock et al, 1999)

2.3.1.3 Barbolini *et al.* (2004)

Similar to Keylock (1999), Barbolini *et al.* (2004) relate the specific loss, SL, to an observed degree of damage:

$$SL = \frac{4DD^2}{64}. \tag{2.5}$$

However, the corresponding impact pressures, p_{imp}, are considerably lower than Keylock's (1999) (Table 2.3). Barbolini *et al.* (2004) proposed the relationship (2.6) (Figure 2.8). They base their proposal on observations from two major avalanche events in Austria, the Wolfsgruben avalanche (St Anton, 18 March 1988) and the Galtuer event on 23 February 1999.

Table 2.3 Degree of damage to buildings (Barbolini et al., 2004)

Degree of damage	**DD**	**p_{imp} (kPa)**	**Phenomena observed**
Moderate	1	5-10	No visible damage to structural elements, damage to frames, windows, etc.
Medium	2	10-15	Failed chimneys, attics or gable walls; damage or collapse of roof
Heavy	3	15-20	Heavy damage to structural elements
Complete	4	>20	Partial or complete failure of the building

$$SL = \begin{cases} 0.0297 p_{imp} & \text{for } p_{imp} < 34\,\text{kPa} \\ 1 & \text{for } p_{imp} \geq 34\,\text{kPa} \end{cases} . \qquad (2.6)$$

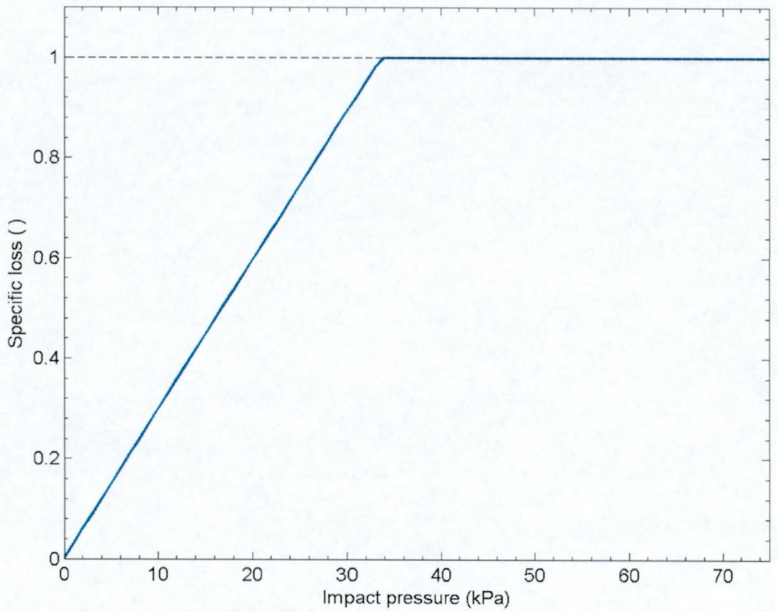

Figure 2.8 Specific loss versus impact pressure (Barbolini et al, 2004)

2.3.1.4 Valentine (1998)

Valentine (1998) evaluated data from nuclear tests to obtain specific loss values as a function of the peak overpressure during explosions. Detailed values of the expected failure of different types of structures are reproduced in Figure 2.9 to Figure 2.15.

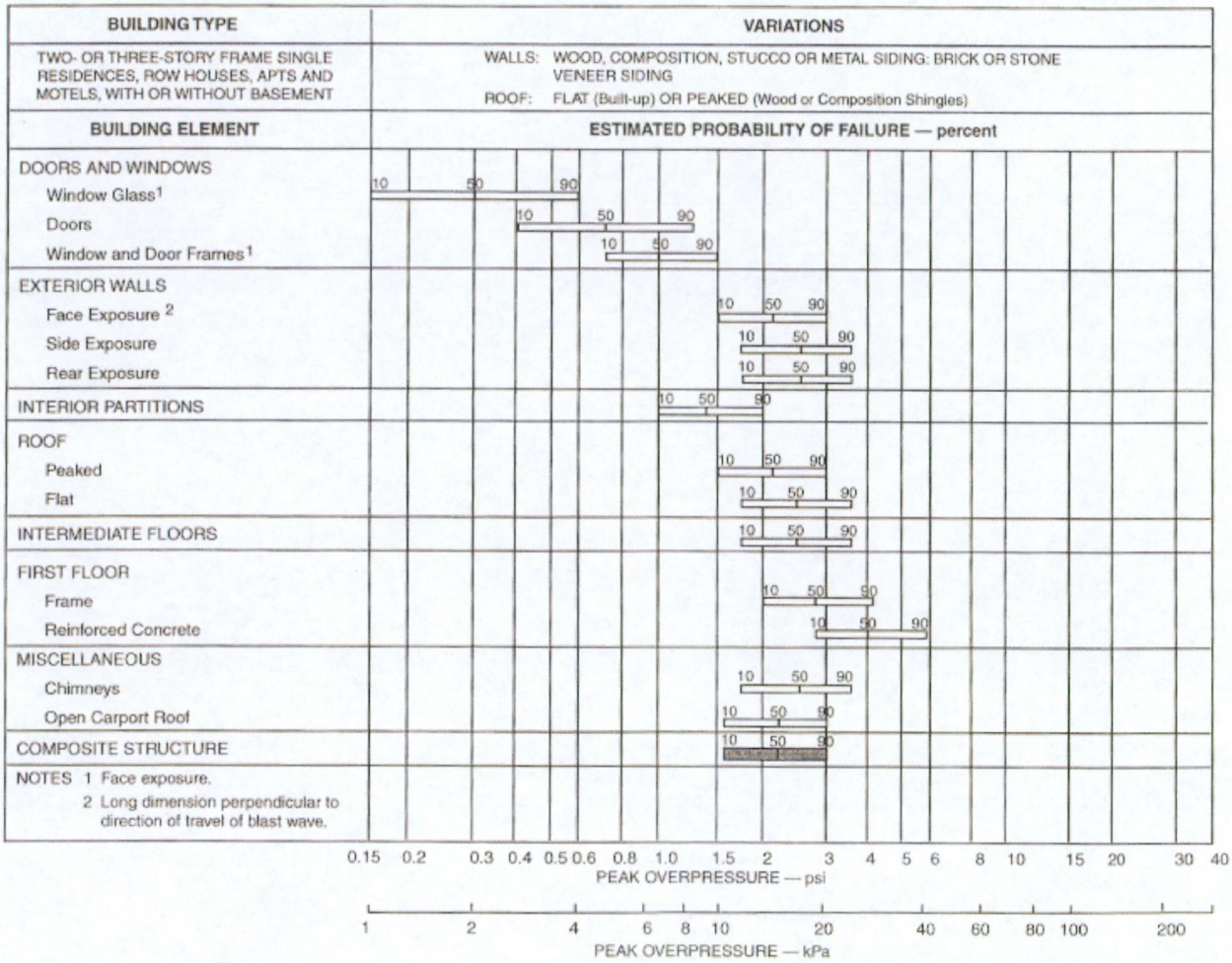

*Figure 2.9 Estimated probability of failure chart for two- or three-story **frame single residences**, row houses, apartments, and motel (From Valentine, 1998).*

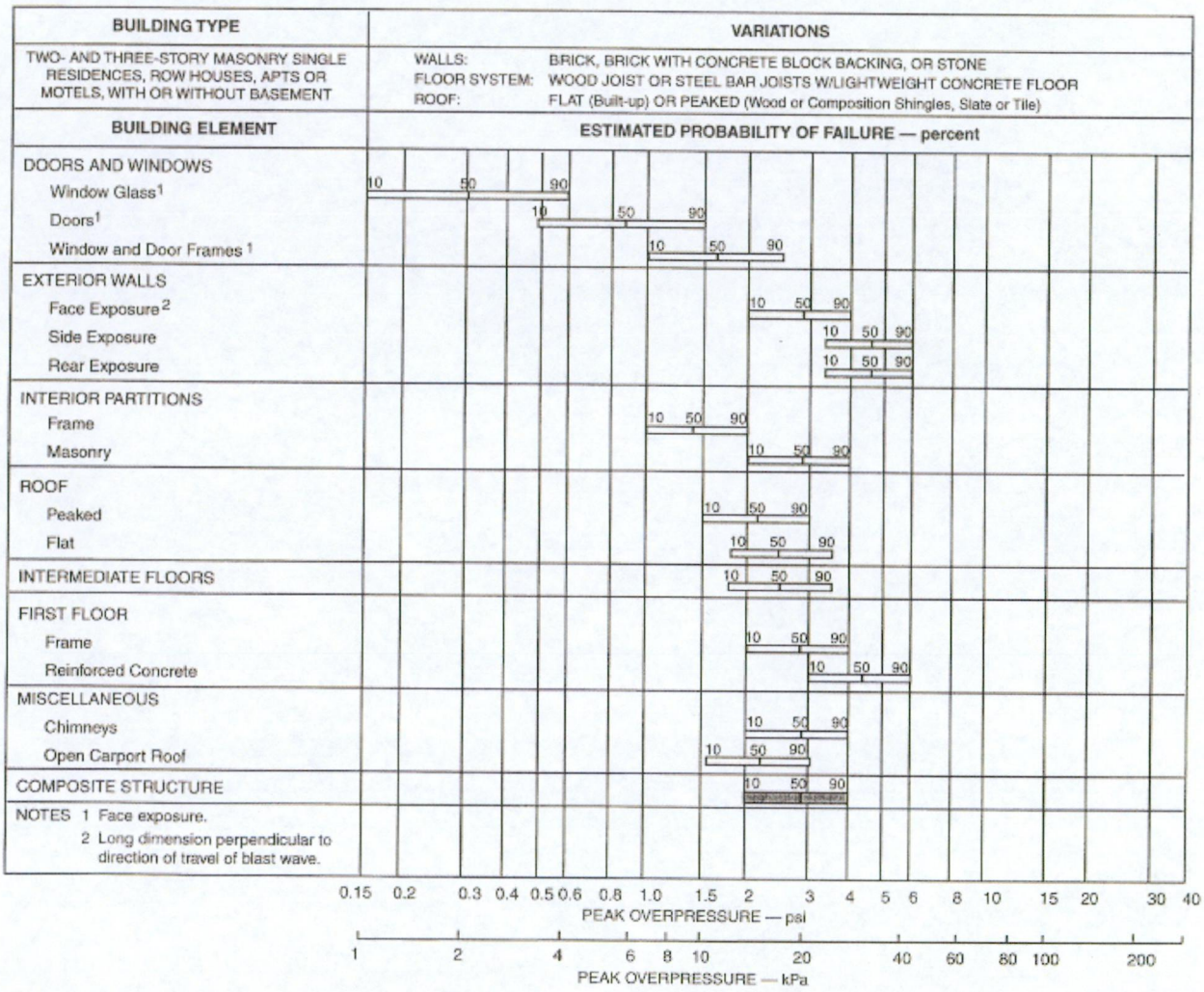

Figure 2.10 Estimated probability of failure chart for two- or three-story masonry single residences, row houses, apartments, and motel (From Valentine, 1998)

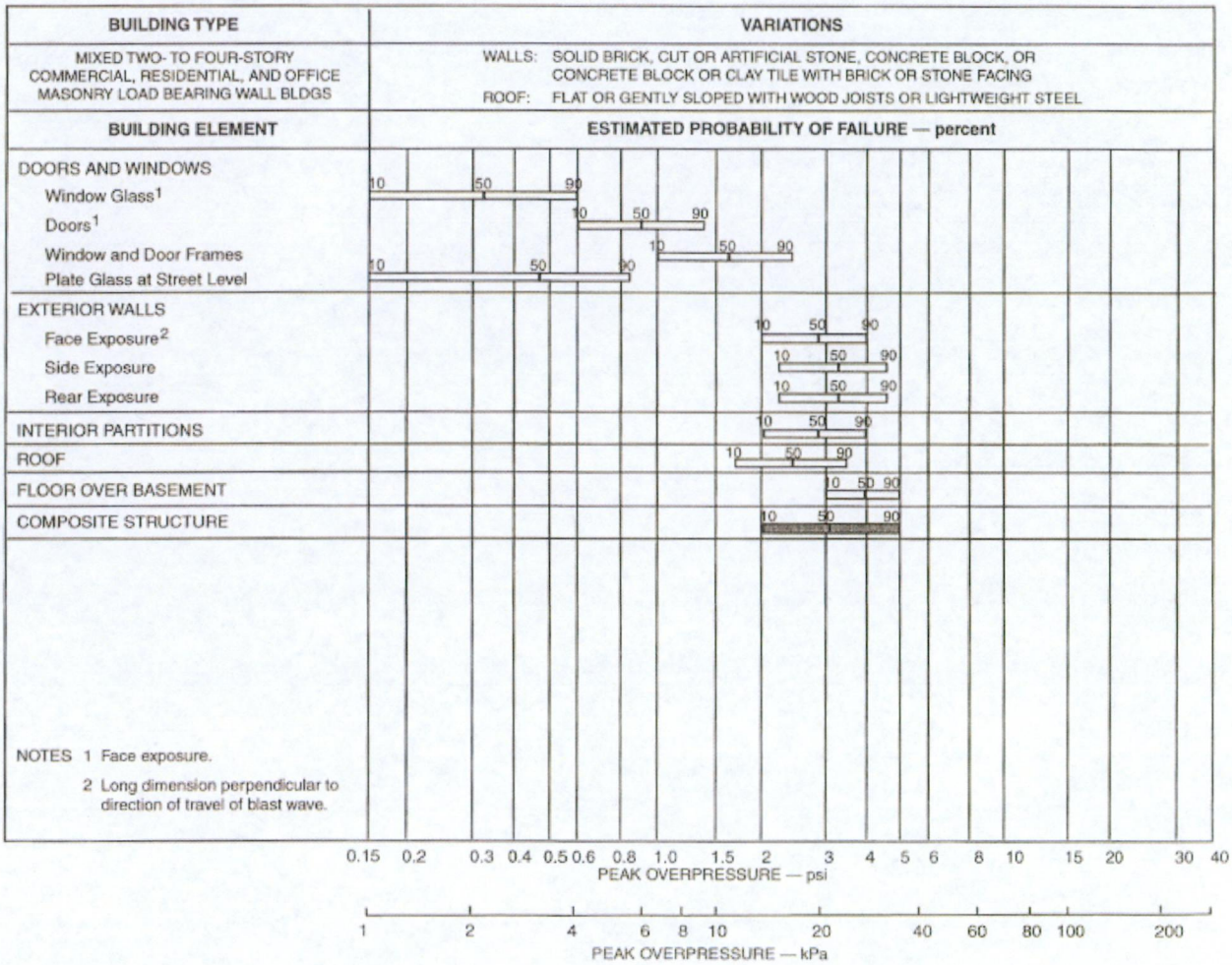

Figure 2.11 Estimated probability of failure chart for ***mixed two- to four-story commercial, residential, and office masonry buildings with masonry load bearing walls****. (From Valentine, 1998)*

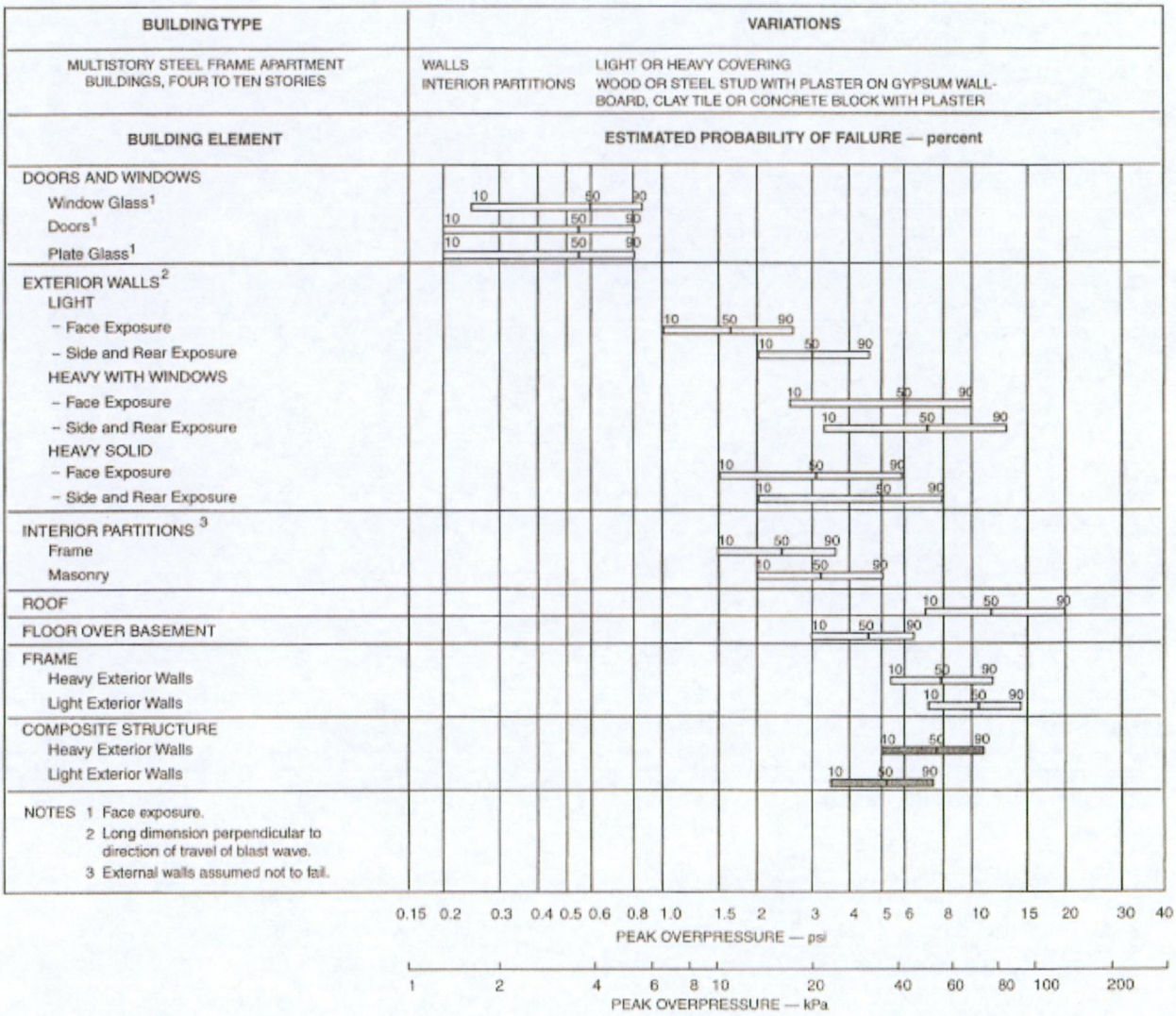

*Figure 2.12 Estimated probability of failure chart for **multi-story steel frame apartment buildings**, four to ten stories high. (From Valentine, 1998)*

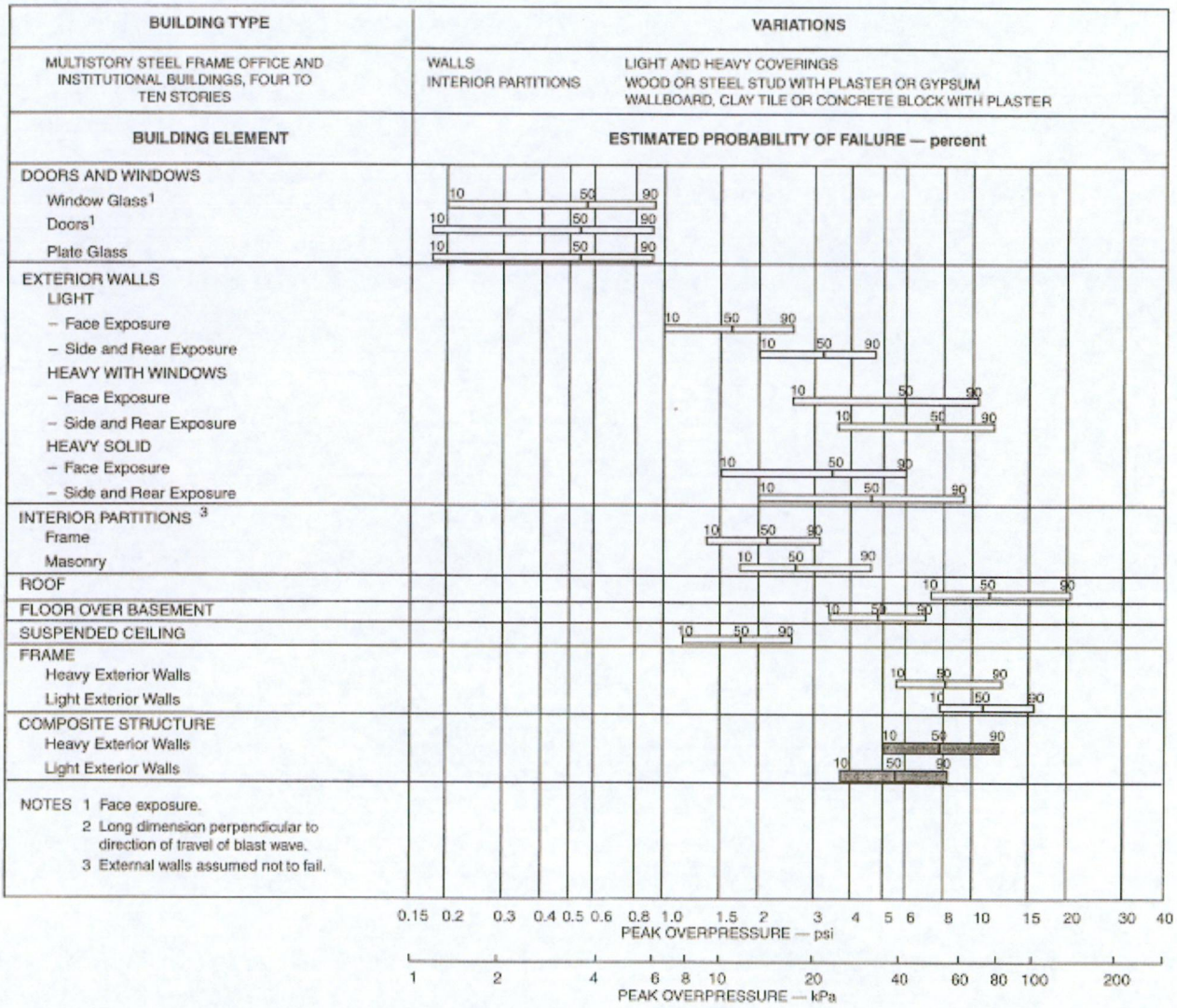

*Figure 2.13 Estimated probability of failure chart for **multi-story office and institutional buildings**, four to ten stories high. (From Valentine, 1998)*

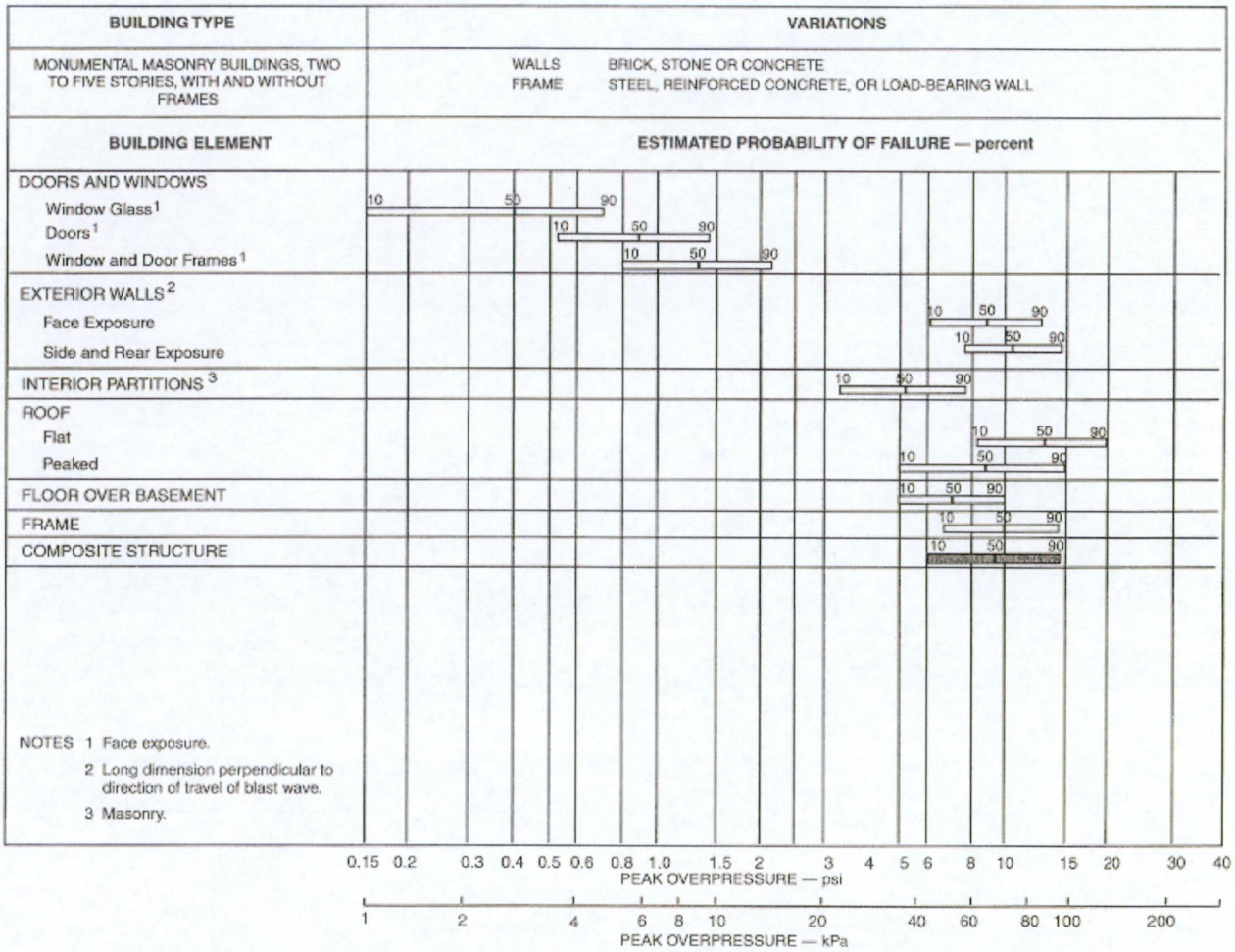

Figure 2.14 Estimated probability of failure chart for ***monumental buildings,*** *two to five stories high. (From Valentine, 1998)*

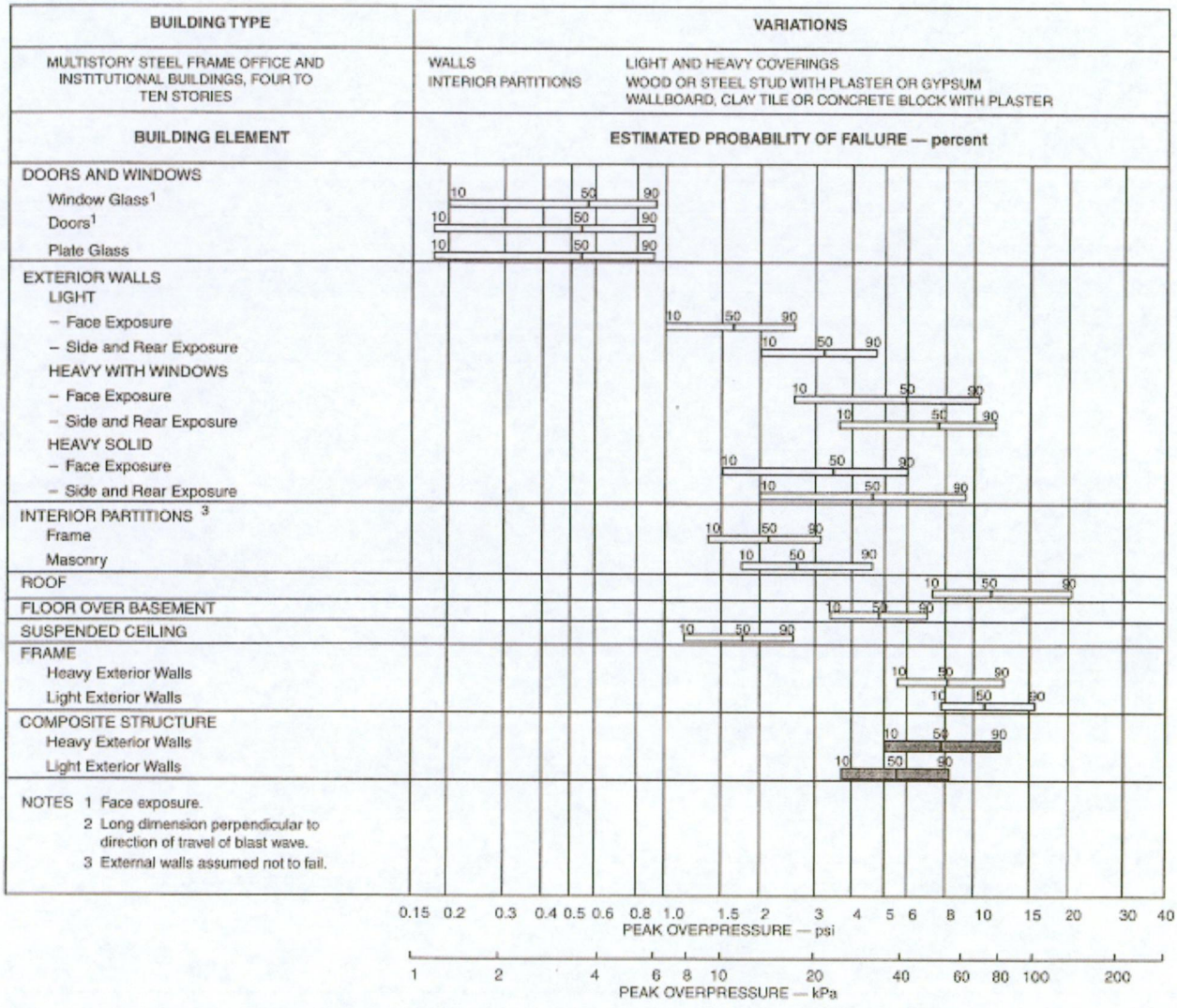

Figure 2.15 Estimated probability of failure chart for ***multi-story frame office and institutional buildings*** *four to ten stories (From Valentine, 1998)*

2.3.1.5 Comparison

Figure 2.16 shows a comparison of some of the proposed specific loss curves.

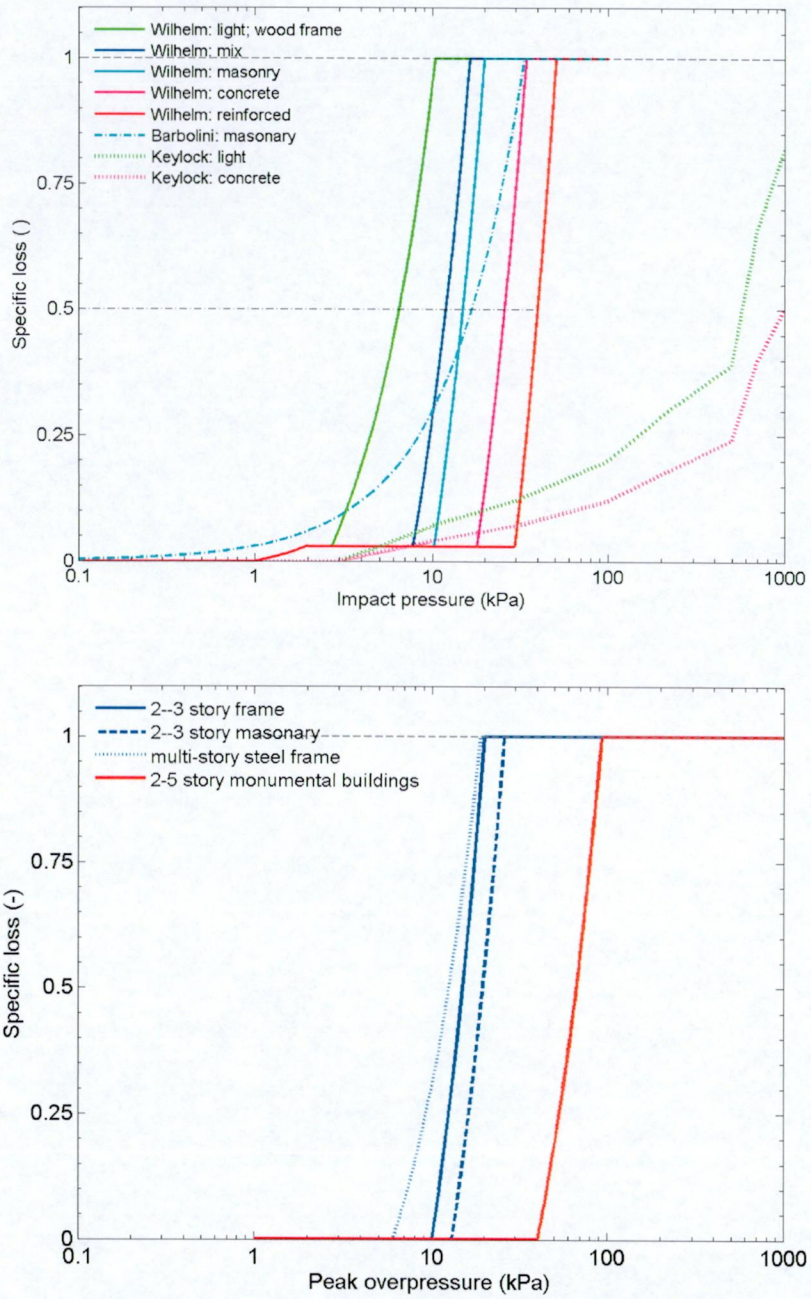

Figure 2.16 Estimated specific loss versus impact pressure; top panel summary of the proposed vulnerability based on avalanche observations (Barbolini et al, 2004; Keylock et al, 2001; Wilhelm, 1999); bottom panel approximations derived for a failure of a exterior wall with face exposure based on (Valentine; 1998).

2.3.2 Persons inside buildings

2.3.2.1 Wilhelm (1997)

Wilhelm (1997) based his vulnerability values (Table 2.4) on data from Switzerland between 1946/47 and 1992/93.

Table 2.4 Vulnerability of persons inside of buildings (Wilhelm, 1997). The data are based on records of 295 persons involved in avalanche events hitting buildings.

Vulnerability			Number of persons
uninjured	0	0.35	104
injured	0<V<1	0.19	56
dead	1	0.46	135

2.3.2.2 Keylock *et al.* (1999)

Keylock *et al.* (1999) tried to derive vulnerability values (fatality probability) for person in buildings and to relate those values to the Canadian avalanche size classification (CASC) (Table 2.5). They distinguished two structure types. However, as for buildings, the pressure assumption behind the CASC is again problematic.

Table 2.5 Probability of death inside a building for two different construction types (Keylock et al. 1999)

CASC	Impact pressure (kPa)	Low-quality construction; wooden frame	Reinforced-concrete Structures
1	1	0	0
1.5	3	0	0
2	10	0	0
2.5	30	0.03	0.02
3	100	0.07	0.04
3.5	220	0.13	0.08
4	500	0.21	0.13
4.5	700	0.33	0.20
5	1000	0.50	0.30

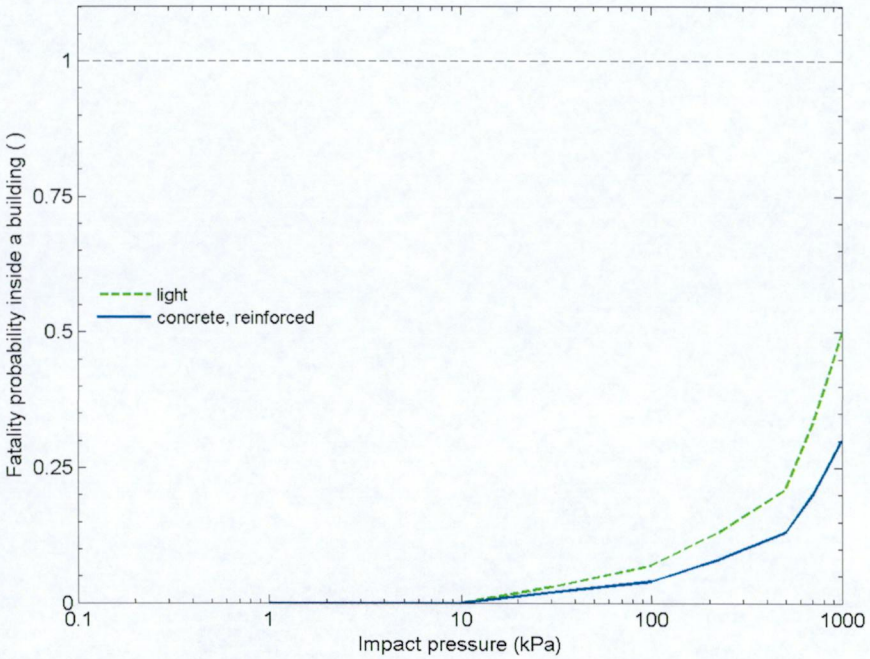

Figure 2.17 Fatality probability versus impact pressure; person inside building (Keylock et al., 1999)

2.3.2.3 Barbolini *et al.* (2004)

Barbolini *et al.* (2004) based their values of fatality probability on observations from two major avalanche events in Austria, the Wolfsgruben avalanche (St Anton, 18 March 1988) and the Galtuer event on 23 February 1999. They found the following relationship between impact pressure and fatality probability, DP_i, of a person inside a building

$$DP_i = \begin{cases} 0 & \text{for } p_{imp} \leq 5\,\text{kPa} \\ 0.0094\,p_{imp} - 0.0508 & \text{for } 5\ \text{kPa} < p_{imp} < 34\,\text{kPa} \\ 0.27 & \text{for } p_{imp} \geq 34\,\text{kPa} \end{cases} \quad (2.7)$$

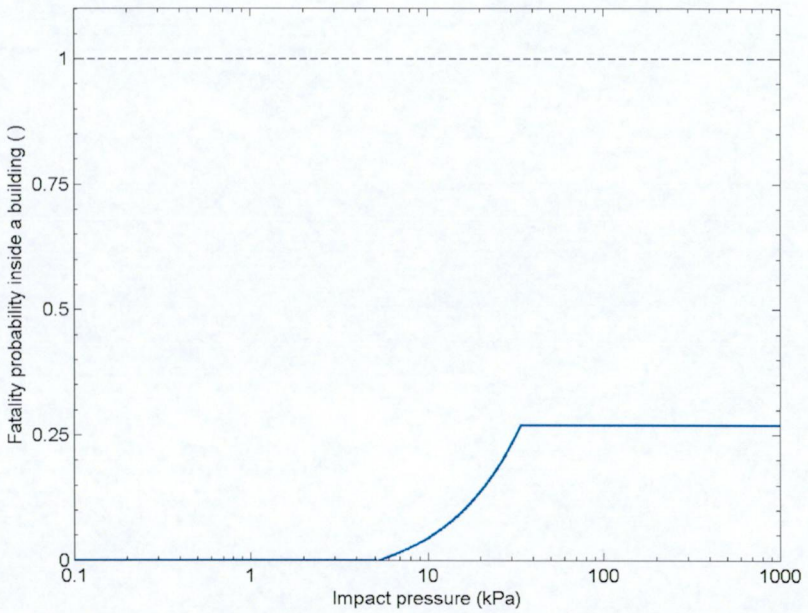

Figure 2.18 Fatality probability of a person inside a building (Barbolini et al, 2004)

2.3.3 Person in car

2.3.3.1 Schaerer (1989) and Hendrikx and Owen (2007)

Schaerer (1989) and Hendrikx and Owen (2007) based their risk assessment on the fatality probability given Table 2.6. They distinguished between different types of slides.

Table 2.6 Vulnerability of a person inside of car, data combined from (Schaerer, 1989) and (Hendrikx and Owen, 2007).

Avalanche class	Estimated impact force per car length (kPa/m)	Fatality probability	Averaged relative impact force of powder snow	Density ρ (kg m^{-3})	Velocity v (m s^{-1})	Flow depth (m)
Powder snow	3.5	0	1	1–15	5–20	> 2.5
Slough	1.7	0	0.5	100–400	1–6	0.2–0.6
Light snow	160	0.05	44	30–250	6–50	0.5–2.0
Deep snow	360	0.25	102	90–300	6–50	2– >2.5
Plunging snow	320	0.50	94	10–100	20–60	> 2.5

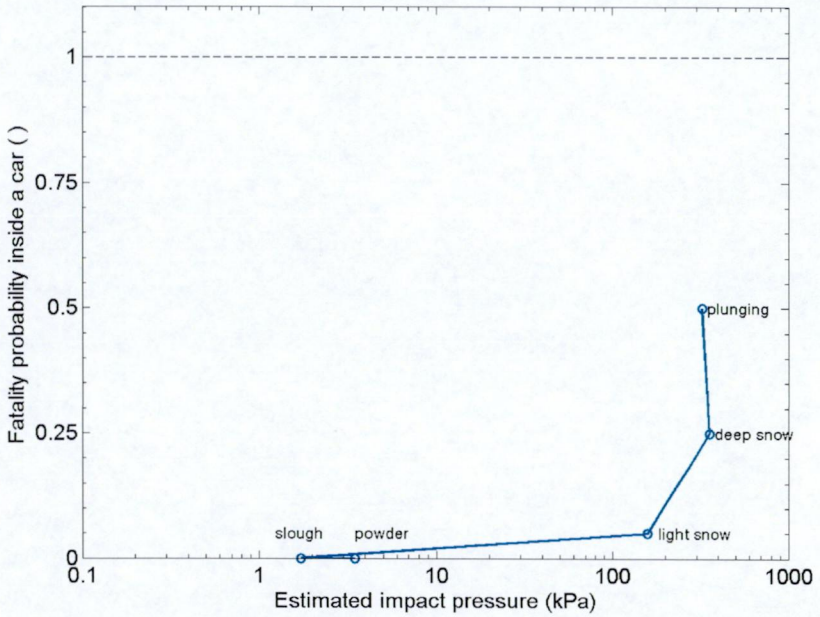

Figure 2.19 Fatality probability of a person inside a car after (Schaerer, 1989).

2.3.3.2 Wilhelm (1997) and Margreth *et al.* (2003)

Wilhelm (1997) based his vulnerability values for persons in a car (Table 2.7) on data from Switzerland between 1946/47 and 1992/93.

Table 2.7 Vulnerability of a person inside a car (Wilhelm, 1997; Margreth et al., 2003). The data are based on records of 129 persons involved in avalanche events hitting cars.

Vulnerability			**Number of persons buried**
total			129 (total)
uninjured	0	0.51	76
injured	0<V<1	0.31	46
dead	1	0.18	27

2.3.4 Persons outdoors

2.3.4.1 Wilhelm (1997)

Wilhelm (1997) based his vulnerability values for persons outside of buildings (Table 2.8) on data from Switzerland between 1946/47 and 1992/93. The data are based on records of 2523 persons involved in avalanche events outdoors.

Table 2.8 Vulnerability of person outdoors (Wilhelm, 1997)

Vulnerability			Number of persons buried
uninjured	0	0.43	1090
injured	0<V<1	0.25	633
dead	1	0.32	800

2.3.4.2 Barbolini *et al.* (2004)

Barbolini *et al.* (2004) based their values on fatality probability on observation from two major avalanche events in Austria, the Wolfsgruben avalanche (St Anton, 18 March 1988) and the Galtuer event on 23 February 1999. The found the following relationship between flow height and fatality probability, DP_o, of a person outdoors

$$DP_o = \begin{cases} 0 & \text{for } h_a < 0.4\,\text{m} \\ 0.0039h_a - 0.1546 & \text{for } 0.4\ \text{m} \le h_a \le 2.1\,\text{m} \\ 0.65 & \text{for } h_a > 2.1\,\text{m} \end{cases} \quad (2.8)$$

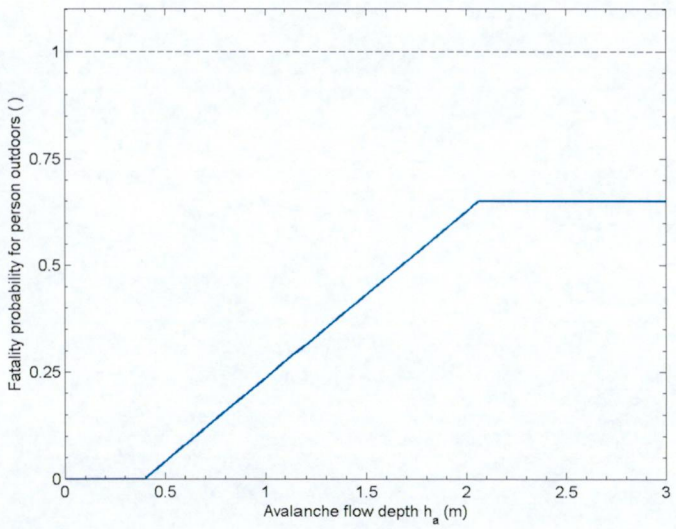

Figure 2.20 Fatality probability of a person outdoors (Barbolini et al, 2004)

2.4 Avalanche risk

Risk is a measure for the probability, or chance, of life and/or material losses. The calculation of avalanche risk at a specific location requires knowledge on:

- the probability that an avalanche release occurs,
- the probability that if the avalanche releases, it actually reaches the location of concern,
- the consequences of the avalanche reaching the location of concern,
- the exposure of the person or object at the location of concern (i.e. the probability that the object or person is present at the location).

2.4.1 Avalanche risk to structures

In the case of risk to a structure, the exposure is usually one and the risk may be written as (e.g. McClung, D. M., 2005)

$$R = \sum R_i \,, \tag{2.9}$$

where

$$R_i = P(C \cap S \cap A) = P(C \mid S_i \cap A) \bullet P(S_i \mid A) \bullet P(A) \,. \tag{2.10}$$

R_i is the risk due to an avalanche of size i and is given by the product of the

- $P(C \mid S_i \cap A)$, the conditional probability of consequence given an avalanche of size S_i
- $P(S_i \mid A)$, the conditional probability of an avalanche of size S_i (or runout distance, respectively; here it s assumed that the runout is correlates with the size.)
- $P(A)$, the probability of an avalanche release.

where C, S, and A stand for the consequence, size of avalanche and avalanche release. This is a multiple magnitude non-product form of the risk equation. The approach requires data or information on magnitude–frequency relationships at a location, which are rarely available. Thus, the single or design event approach (.i.e., a conjectural avalanche of predefined return period, e.g. 300 years) as is used instead, that is the risk is calculated

$$R_d = P(C \cap A_d) = P(C \mid A_d) \bullet P(A_d) \,, \tag{2.11}$$

where

- $P(C \mid A_d)$ is the conditional probability of consequence of the design avalanche
- $P(A_d)$ is the probability of occurrence of the design avalanche at the location.

However, this "design event" approach tends to underestimate the risk, as it was seen for the probability approach in the example in Section 2.2 for the avalanche hazard.

2.4.2 Avalanche risk on traffic roads

In the case of road traffic, the exposure is highly variable and may have a huge influence on the risk. Kristensen *et al.* (2003) propose the following risk equation to calculate the collective risk, CR, due to an infrequent avalanche on a road:

$$CR = \beta \, \lambda \frac{ADT}{24} \frac{(L + B_d)}{v} f_a \text{ fatalities per year,} \tag{2.12}$$

where

- ADT Average traffic volume for avalanche period per day
- V Speed of vehicle (km/h)
- λ Probability of death in a vehicle hit by an avalanche
- β Mean number of passengers per vehicle
- L Width of avalanche = average length of road covered by the avalanche (km)
- B_d Stopping distance ($B_d = (V/3.6)^2/8000$) in km
- f_a Avalanche frequency ($f_a = 1/T_r$; T_r is the return period)

Similar equations were proposed by (Wilhem, 1997) or (Margreth *et al.* 2003). Schaerer (1989) and Hendrikx and Owens (2007) presented an extended equation including multiple avalanche paths and waiting traffic:

- Collective Risk (fatalities per year), IR_w including waiting time

$$CR_w = \frac{\beta}{24} \sum_{j=1}^{5} \lambda_j \sum_{i=1}^{N_a} \left(\frac{ADT\left(L_{ij} + B_d\right)}{v\,TR_{ij}} + P_s \sum_{k=1}^{N_b} \frac{NW_{ik}\, d_k}{TR_{kj}} \right) \tag{2.13}$$

- Individual Risk (fatalities per year) CR_w including waiting time

$$IR_w = \frac{z}{24} \sum_{j=1}^{5} \lambda_j \sum_{i=1}^{N_a} \left(\frac{ADT\left(L_{ij} + B_d\right)}{v\,TR_{ij}} + P_s \sum_{k=1}^{N_b} \frac{NW_{ik}\, d_k}{TR_{kj}} \right) \tag{2.14}$$

where:

- CR Collective risk (deaths per year)
- ADT Average traffic volume for avalanche period per day
- β Mean number of passengers per vehicle (β_B for busses, β_C for cars)
- N_a Number of avalanche paths
- L_i Width of avalanche = average length of road covered by avalanche i (km)
- R_i Return period for avalanche i (years) (from avalanche database)
- v Speed of vehicle (km/h)
- B_d Stopping distance (= (ucar/3.6)2/8000 (km), where ucar is the car speed
- λj Probability of death in a vehicle hit by an avalanche type j
- IR Individual probability of death per year
- z Number of passages per day of that person
- j Avalanche type for j=1 to 5 (Table 2.6 for the type definition
- w Subscript to indicates that waiting traffic is accounted for
- k Number of numbering path

- Ps Probability that an secondary avalanche will run along path k while the traffic is waiting
- NWik Number of vehicles exposed to adjacent avalanche path, k of path i
- NWTik Number of vehicles exposed to adjacent avalanche path, k of path i in time period dk.
- dk Length of time waiting vehicles are exposed to an avalanche in the adjacent path
- TRij Return period of occurrence of adjacent avalanches of type j at the avalanche path k given in years.

Actually, Hendrikx and Owens (2007) disregarded the contribution from the stopping distance B_d.

Hendrikx and Owens (2007) proposed a set of typical values for the parameters, which are summarized in the following table.

Table 2.9 Summary of parameter values given by Hendrikx and Owens (2007).

Parameter	Value	Remarks
β_B	30	
β_C	1.6	
$\lambda[i]$	[0.05; 0.25; 0.5; 0.5; 0.5; 0.5]	
z	2	for commuter
z	6	for road crew member
P_s	0.15	

3 CASE STUDY ZONING: FARM WITHIN IN AN AVALANCHE PATH

3.1 Introduction

A farm is located at the foot of an avalanche path at about 30 m asl. Main features of the avalanche track are as follows. The terrain behind the farm climbs up to approximately 1500 m; between 1300-1500 m, there is a glacier field with a slope of about 20°. At an altitude between 1300 down to-1200 m, the slope angle is about 30°. Between 550 m asl and 300 m asl there is a 1300 m long "plateau" with an slope angle of about 11° before the terrain steeps again down to sea level. There, the slope angle is around about 20°. The mean slope angle of the total avalanche track is approximately 19.9°. A profile of the track is given in Figure 3.4. The farm dates back to the 13th century and no avalanches where recorded to runout as far down as to the farm.

3.2 Avalanche Hazard

3.2.1 Meteorology parameter: precipitation

It is widely recognized (Bakkehoi, 1987; McClung and Schaerer, 2006) that one of the most important meteorological parameters relevant for the release of catastrophic avalanches is the 3-day precipitation accumulation. Assumed return periods for the 1, 3 and 5-day new snow sum, HNS, are shown in Figure 3.1.

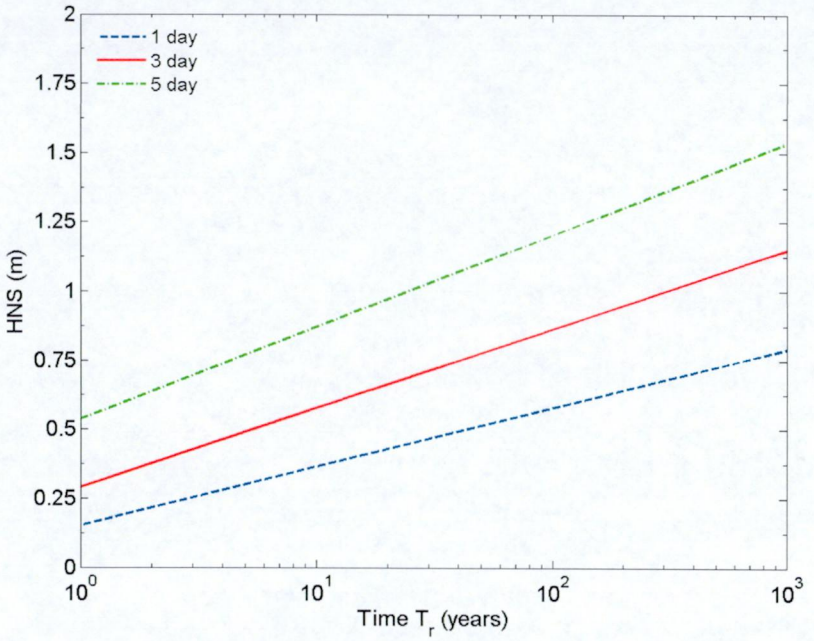

Figure 3.1 Return period of HNS(1d), HNS(3d), and HNS(5d) (new snow accumulated in 1, 3 or 5 days, assuming a snow density ρ = 150 kg m^{-3}). $1/T_r$ is approximately the occurrence probability (estimated curve).

3.2.2 Release model

Following Lackinger (1989) and Harbitz *et al.* (2001), a simple snow-slab avalanche model is assumed (Figure 3.2). The acting forces are the weight, W, of the slab, the tension force, F_T, at the crown, the compression force, F_C, at the stauchwall, the flank force, F_F, and the shear force, F_S, along the shear surface. The width of the slab is B and its length L. These forces can be estimated from the following equations:

$$\begin{aligned} &W = \rho g BLD + W_{ext},\ T = W\sin\psi,\ F_T = BD\sigma_t, \\ &F_c = BD = 2BDY_{DM}(1+\rho gD/Y_{DM}), \\ &F_F = 2LDc,\ F_S = BL\tau_S \end{aligned} \tag{3.1}$$

The stress and the slide thickness, D, are give by

$$\begin{aligned} \sigma_t &= 0.5 Y_{DM} \\ \sigma_c &= Y_{DM} \\ \tau_c &= \frac{Y_{DM}}{\sqrt{3}} \\ D &= \Delta HS \cos(\psi) \end{aligned} \tag{3.2}$$

ΔHS, is the depth of the slide measured vertical and the yield strength is approximated by

$$Y_{DM} = 2.1 \times 10^{\left(\frac{\rho - 100}{150}\right)} \text{ [kPa]} \tag{3.3}$$

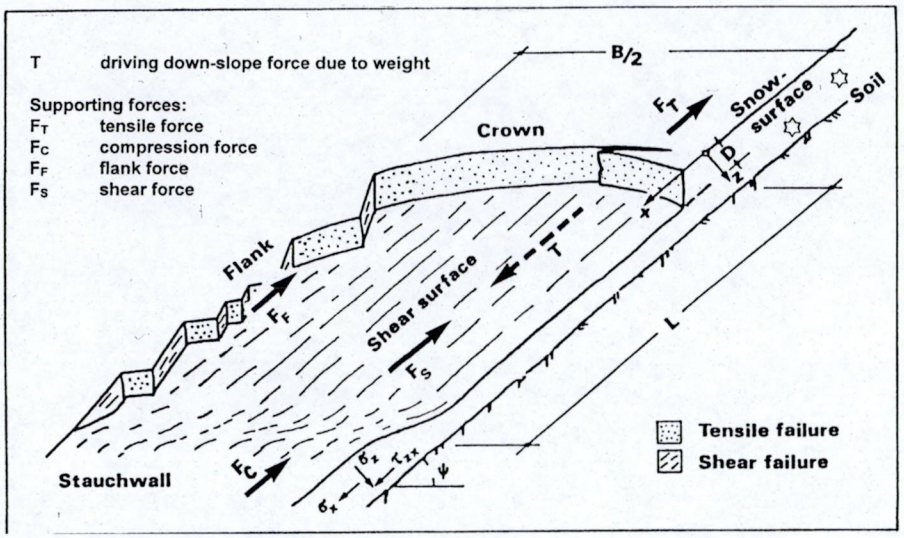

Figure 3.2 Snow-slab avalanche definitions, coordinate system and acting forces (Lackinger, 1989).

Monte-Carlo simulation can also be applied to examine the probability of release for a given (3-day) new snow depth. Figure 3.3 compares the model results with results of observations at five Norwegian sites (Bakkehoi, 1987). The SF line gives the boundary for a deterministic calculation using the mean values. The used probability distributions of the basic random variables are summarized in Table 3.1. In the calculation, the additional external load, W_{ext}, is disregarded. However, it might be reasonable to include W_{ext} to account for increased loading due to, e.g., blowing and drifting snow.

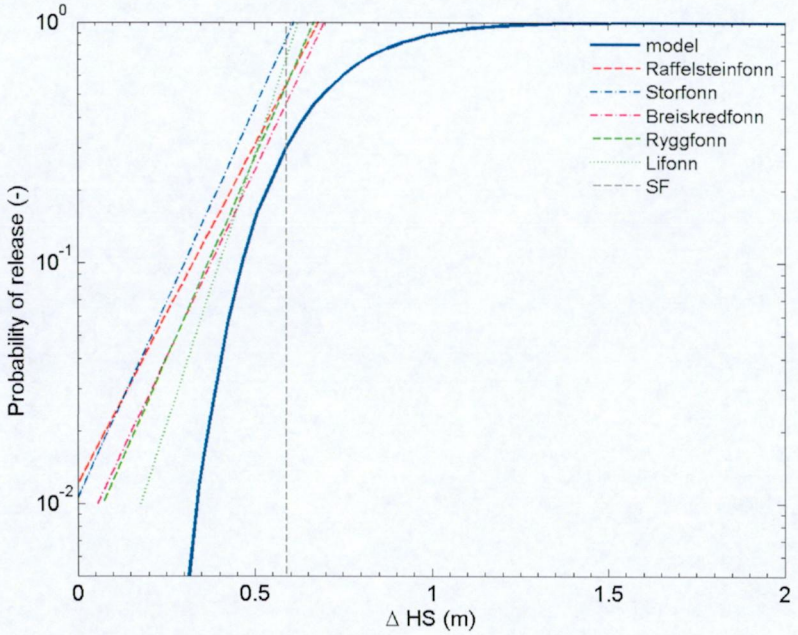

Figure 3.3 Probability of snow slab release for given slab depth, ΔHS, above a weak layer.

Table 3.1 Probability distribution of the basic random variables in the avalanche slide model.

Random variable	**Distribution**	**Mean**	**Standard deviation**
Thickness (or height) of slab, D	Beta	$\Delta HS \cos\psi$	$0.2\ \Delta HS \cos\psi$
Slope angle, ψ	Lognormal	31°	2.2°
Shear strength of sliding plane, τ_s	Lognormal	400 Pa	$0.5\ \tau_s$
Width of slide, B	Normal	200 m	0.1 B
Length of slide, L	Normal	150 m	0.1 L
Density of snow, ρ	Lognormal	150 kg/m^3	$0.1\ \rho$
Additional load W_{ext}		0	0

3.2.3 Slide runout model

After an avalanche release, the probability of the avalanche to reach a specific location is of interest. To completely answer this question, in-depth understanding on avalanche dynamics is required. However, dynamic models often use oversimplifications. Another, possibility is to use statistical run-out models like the α-β model (Bakkehoi *et al.* 1983); another is to use an energy line approach (Körner, 1980). This example follows the energy line approach combined with a Monte-Carlo simulation. Based on simple energy considerations, the energy line approach allows to determine the runout length and to give an estimate on the velocity along the track (Figure 3.4):

Kinetic energy = loss of potential energy – energy loss due to friction

or

$$\frac{v^2}{2g} = \Delta H - \mu L\,, \tag{3.4}$$

where ΔH is the elevation drop along the track, L the horizontal travel distance, v the avalanche speed, and μ is the so-called runout ratio (i.e. is a measure of the frictional loss). The runout is defined by the intersection between profile line and the energy line given by

$$z = z_0 - \mu(x - x_0)\,, \tag{3.5}$$

where (x_0, z_0) are the coordinates of the release location.

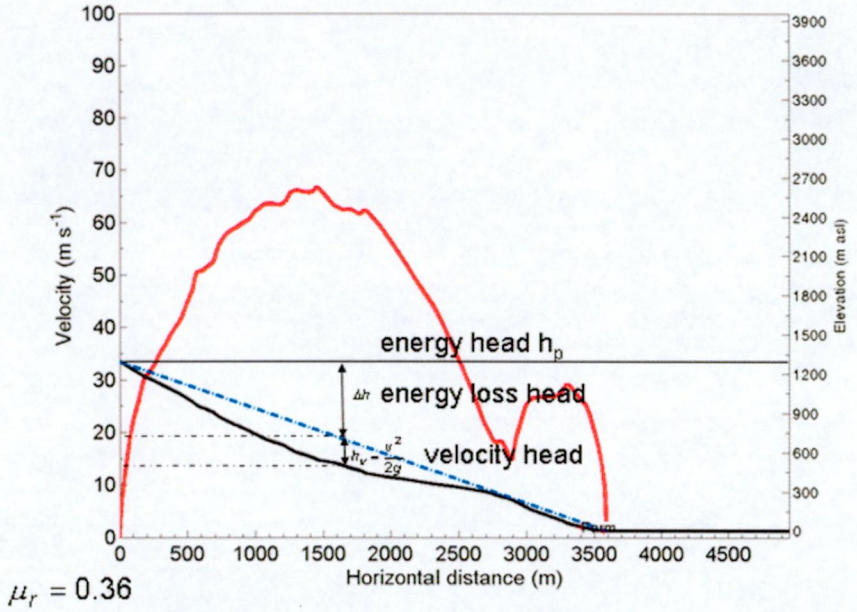

Figure 3.4 Energy line approach. The energy head marks the initial potential energy. The red curve indicates the difference between initial energy and energy loss due to friction. (The estimated velocity in the example is: $v = \sqrt{2gh_v} \approx 65\,\mathrm{m\,s^{-1}}$*.)*

Figure 3.5 depicts the probability that an avalanche runs out to a point along the track. The figure shows the result of a Monte-Carlo simulation using μ as a random variable (Table 3.2). The probability that the avalanche reaches the farm (x = 3455 m) is about 0.11. The probability distribution of the avalanche speed, v_a, at the horizontal distance x = 3455 m is shown in Figure 3.6.

Table 3.2 Probability distribution of the basic random variable, μ, in the avalanche runout model.

Random variable	Distribution	Mean	Standard deviation
Runout ratio μ	lognormal	0.4	0.1

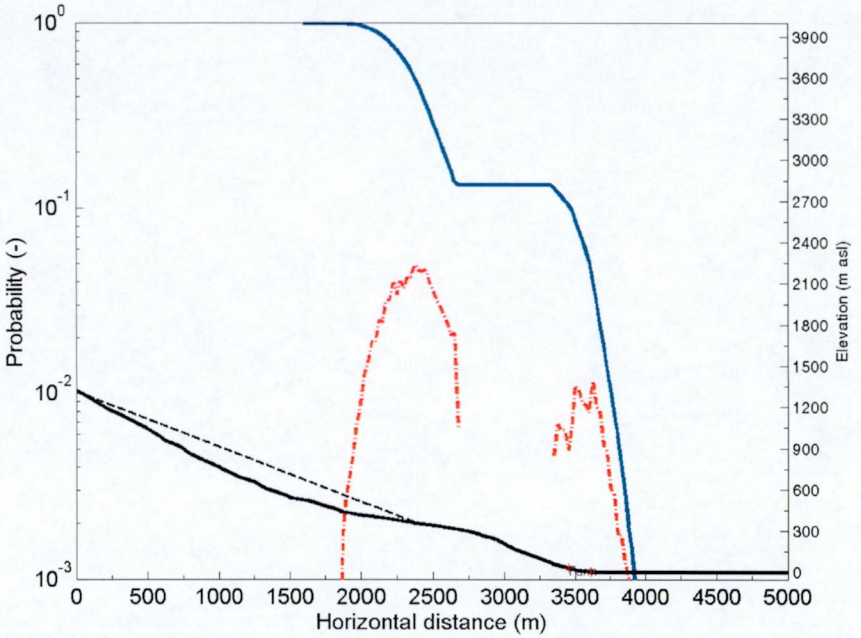

Figure 3.5 Probability of horizontal travel distance is given by the blue curve. The red dashed curve shows PDF of where the avalanche stops.

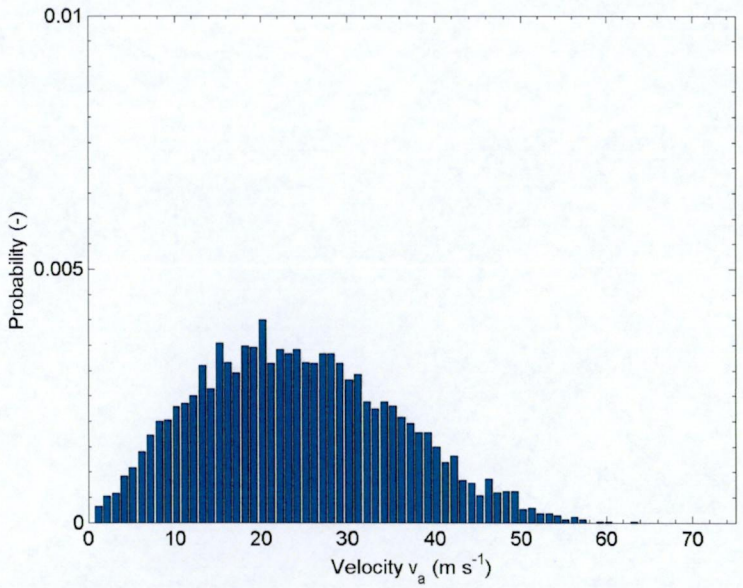

Figure 3.6 Probability $P(v-\Delta v< v_a < v)$ of avalanche speed ($v_a > 0$) at the farm location (point x = 3455 m).

3.2.4 Hazard value

The probability to observe a slide release is integral of the conditional probability of slide release assuming an additional snow depth, ΔHS_0, above a potential sliding plane, times the probability that ΔHS_0 occurs over all possible ΔHS.

$$P_{slide} = \int_0^\infty P(\text{Release} \mid \Delta HS < \Delta HS_0) \bullet P(\Delta HS = \Delta HS_0)\, d\Delta HS\,. \tag{3.6}$$

As approximation, one obtains

$$P_{slide} = \sum_{i=1}^{n} P_i(\text{Release} \mid \Delta HS < \Delta HS_0) \bullet P_i(\Delta HS = \Delta HS_0) \bullet \Delta hs \approx 0.011\cdot \tag{3.7}$$

where Δhs is the width of the discrete snow depth increment.

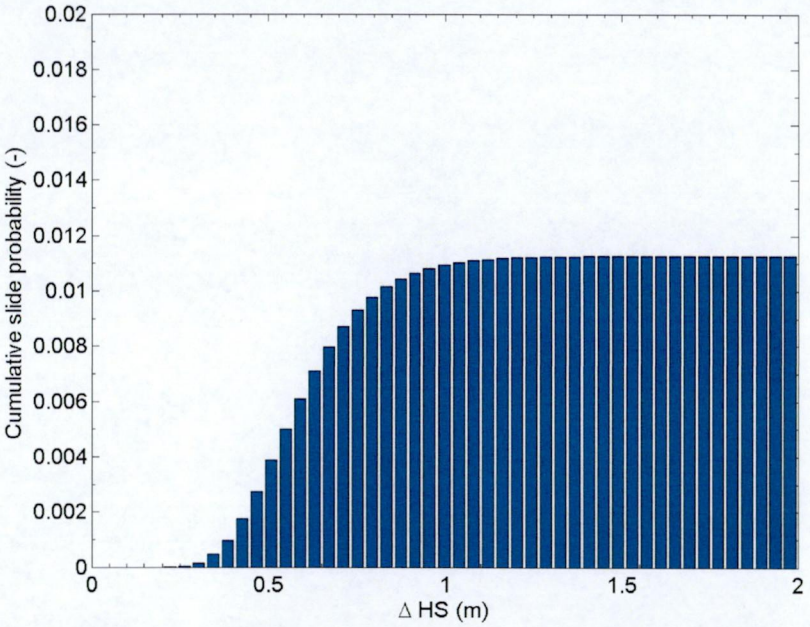

Figure 3.7 Cumulative probability slide occurrence for given new snow depth ΔHS above a weak layer.

The avalanche hazard at farm location (point x = 3455 m) is given by the probability of the avalanche occurrence times the probability that the avalanche actually reaches the location:

$$H = P_{slide}\, P_{travel} \approx (0.011)(0.11) \approx 1.2\cdot 10^{-3} \text{ per year.} \tag{3.8}$$

This hazard is slightly higher as that what the Norwegian building code requires for domestic building or cabins ($<1\cdot 10^{-3}$ per year). The probability that no avalanche reaches the farm in t =700 years is

$$P = e^{-1.2\cdot 10^{-3} t} \approx 0.4\,. \tag{3.9}$$

3.3 Vulnerability

The vulnerability of a building at point x = 3455 m is defined by the integral of the conditional probability of specific loss assuming an avalanche speed v_a times the probability that v_a is realized over all possible speeds.

$$V = \int_0^\infty P(\text{loss} \mid v < v_a)\, P(v_a = v)\, dv\,. \tag{3.10}$$

As an approximation, one obtains

$$V = \sum_{i=1}^{n} P_i(\text{loss} \mid v < v_a)\, P_i(v - \Delta v < v_a < v) \approx 0.098\,. \tag{3.11}$$

For a constant avalanche density ρ_a = 200 kg m^{-3}, the impact pressure, p_{imp}, on a building can by estimated by

$$p_{imp} = \rho_a v^2\,. \tag{3.12}$$

The assumed specific loss is shown in Figure 3.8. This specific loss curve is similar to those given by (Valentine, 1998) for wooden frame buildings (Figure 2.16). Figure 3.8 depicts the cumulative vulnerability curve for a given avalanche velocity.

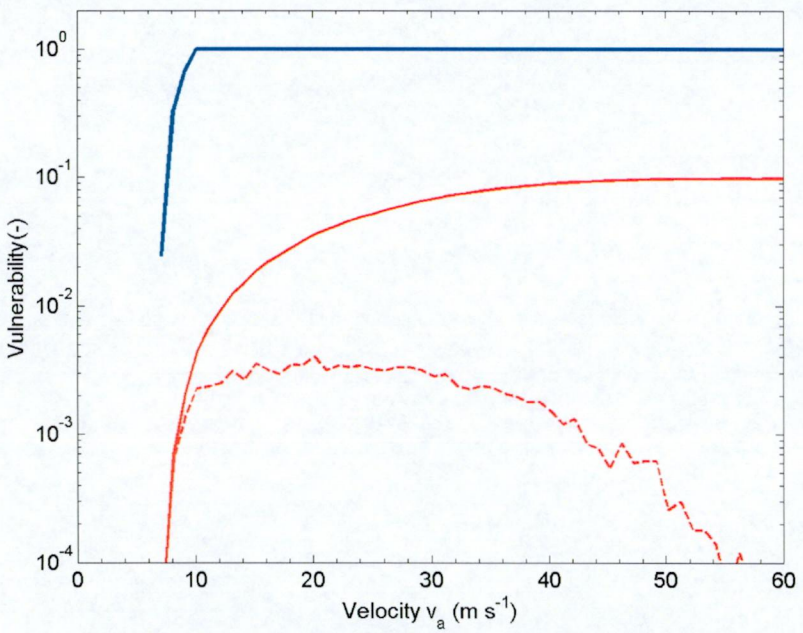

Figure 3.8 Cumulative vulnerability curve versus avalanche speed (red solid line); red dashed curve depicts corresponding PDF. The blue line shows assumed specific loss curve for a wooden frame building.

Assuming a constant density is a crude simplification, and observations actually indicate that the flow density (i.e. the density of the avalanche in motion) decreases with increasing avalanche velocity. Assuming a simple relationship

$$\rho_{ma} = \rho_0 - a_\rho \max(0, \min(1, (v_a - v_l)/(v_u - v_l))), \quad (3.13)$$

where ρ_{ma} is a mean random flow density. A density distribution is given in Table 3.3.

In this case, the impact pressure is approximated by

$$p_{imp} = \rho_{ma} v^2. \quad (3.14)$$

This modification actually increases the cumulative vulnerability slightly to V = 0.1 in the example due to the higher flow density at low speeds.

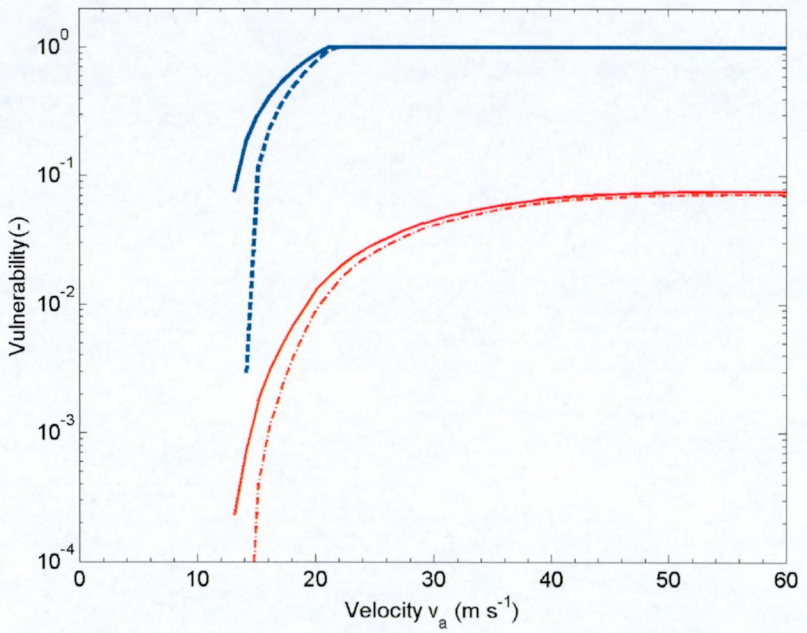

Figure 3.9 Cumulative vulnerability curve versus avalanche speed (red solid line velocity dependent density; red dashed line constant flow density). The blue lines show corresponding specific loss curve for a monumental buildings.

This modification leads to a modified vulnerability curve (Figure 3.9) for, e.g., a monumental building. The difference in this case is largest at low velocities due to the assumed velocity distribution. Observations suggest that avalanche densities decreases with increasing avalanche velocity; this would mean that difference will be more obvious at location were the avalanche passes with high speeds. An example of this behaviour is shown Figure 3.10. Here, at low avalanches velocities the vulnerability for the variable density is larger, but above a certain velocity, it is less than for the case of constant density. This can be of interest in the case of, e.g., power lines in an avalanche.

Table 3.3 Probability distribution of the flow density as random variables in the vulnerability model.

Random variable	Distribution	Mean	Standard deviation
Flow density, ρ_a	Lognormal	$\rho_{ma}(v_a)$	0.1 $\rho_{ma}(v_a)$

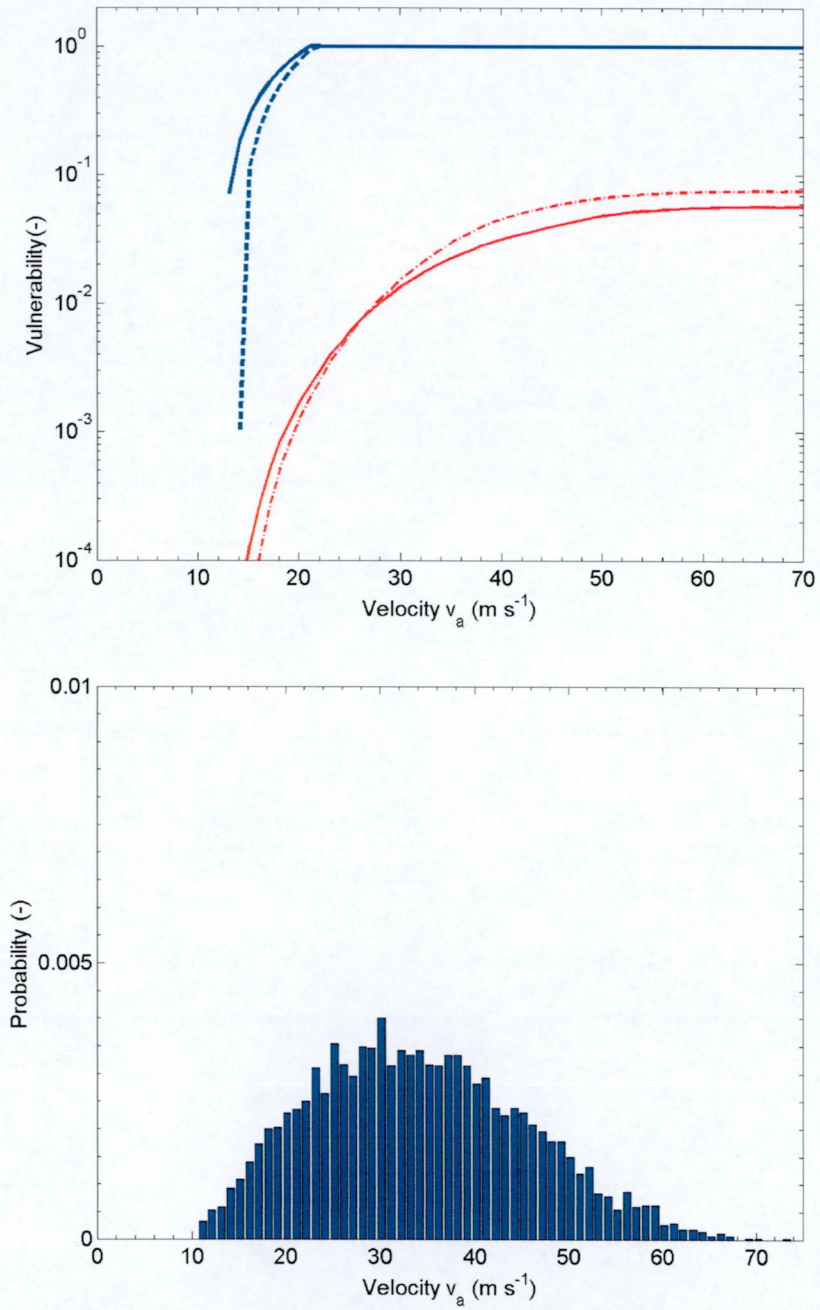

Figure 3.10 Cumulative vulnerability curve versus avalanche speed (red solid line velocity dependent density; red dashed line constant flow density). The blue lines show corresponding specific loss curve and the lower panel the corresponding velocity distribution.

3.4 Risk

3.4.1 Building

The risk to a building is given by the product of slide occurrence (hazard) times the vulnerability of the specific building.

$$R_{loss} = P_{slide} \bullet V \approx (0.011)(0.098) \approx 1.1 \cdot 10^{-3}. \tag{3.15}$$

In this case, we followed a multiple magnitude approach. For comparison, let us take a single (design) event approach. Assuming the avalanche release at a new snowdepth of about 0.6 m (deterministic), we obtain 3-day return period of approximately 12 year or a slide release probability 0.08 per year, which is for our example about 7 times higher than the presented Monte-Carlos approach suggests. Simulations of the design avalanche using an avalanche model (PCM-model (Perla *et al.*, 1980); NIS-model (Norem *et al.* 1987)) suggest a speed of 20 to 40 m s^{-1} at the farm location. In this case, the vulnerability equals one and the risk is $R_{loss} = 0.08$. The huge discrepancy in this example between the multiple magnitude approach and the design avalanche approach originates from the neglecting the probability with respect to the travel distance, P_{travel}.

3.4.2 Inhabitants

The individual risk to a person is given by the product of probability of slide occurrence (hazard) times the probability that the slide reaches the location times the vulnerability (probability of death) times the exposure of the respective person:

$$\begin{aligned} IR &= P_{slide} \bullet P_{travel} \bullet P_{kill} \bullet P_{\exp} \\ &\approx (0.011)(0.11)(0.46) \bullet P_{\exp} \approx 1.3 \cdot 10^{-3} \bullet P_{\exp} \end{aligned} \tag{3.16}$$

where P_{exp} is the probability that a specific person is present during the release (i.e. the exposure). For a person that occupies the house during 10 hours a day, the individual fatality risk 5.4×10^{-4} per year. Assuming a lifetime of 80 years the person has a probability of about 0.04 to die due to an avalanche during his life span.

Assuming a family of five person (N_p =5), which are on average 8 hours per day in the building (P_{exp} = 0.333), we obtain a collective risk of

$$\begin{aligned} CR &= N_p \bullet P_{slide} \bullet P_{travel} \bullet P_{kill} \bullet P_{\exp} \\ &\approx (5)(0.011)(0.11)(0.46)(0.333) = 9.3 \cdot 10^{-4} \text{ fatalities per year} \end{aligned} \tag{3.17}$$

Considering the age of the farm there is a probability of 0.65 avalanche fatalities during the 700 years period.

4 CASE STUDY ROAD RISK: EXAMPLE N15 GRASDALEN

4.1 Introduction

RV15 is located in western Norway and is an important transportation corridor for the region. Alternative routes are long and require the use of ferries. There is no alternative railway and 12 express busses use the road daily. Heavy truck traffic is required for "just-in-time" production at the west coast. In winter, several avalanche paths that constitute a considerable hazard endanger the highway.

The example looks at the risk to people trapped by an avalanche and in waiting traffic. The calculation also shows the benefit of a protection gallery at parts along the road.

4.2 Overview of the area

Figure 4.1 gives an overview of the whole stretch and the location of severe avalanches at Grasdalen.

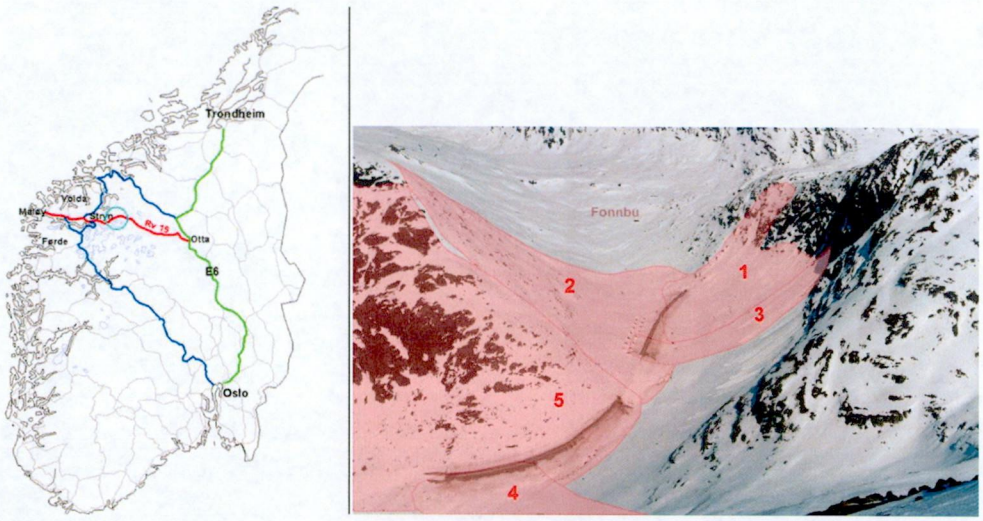

Figure 4.1 Overview map of RV15 (left). The circle indicates the location of Grasdalen where five avalanche paths endanger the road (right).

4.3 Data collection

4.3.1 Traffic volume

Table 4.1 summarizes the traffic situation and the vulnerability assumed in the calculations.

Table 4.1 N15 collected data

Type	ADT	Averaged velocity v (m s^{-1})	Stopping distance (m)	Mean number of passengers, β	Vulnerability λ
Car	800	17	35	1.6	0.36
Bus	12	17	35	30	0.36

4.3.2 Description of avalanche path

Figure 4.2 depicts the expected number of avalanches events per 20 m interval along the endangered stretch at Grasdalen. For the calculations, a simplified model of five separate "avalanche paths" is assumed. The characterization is given in Table 4.2. The star marks the assumption for the case that the present gallery is disregarded. This is down to evaluate the effect of the gallery.

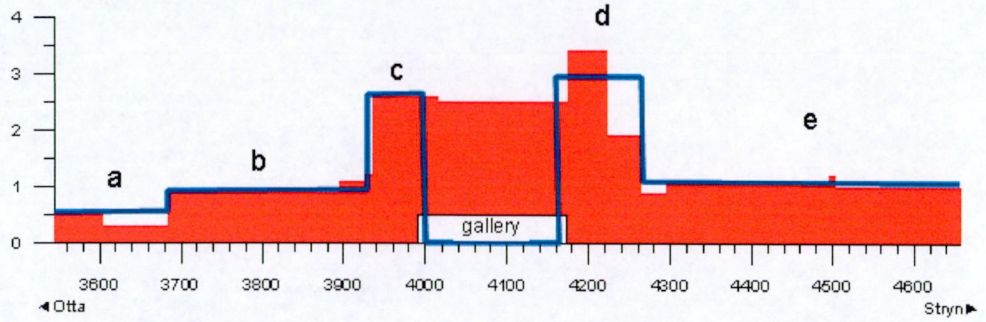

Figure 4.2 Number of events per year along the endangered stretch at Grasdalen. The blue line depicts the simplified model.

Table 4.2 Grasdalen avalanche path characterization (c marks the situation without the gallery).*

Path	length (m) L_i	Avalanche frequency per year ($f_{ai} \approx 1/TR$)	Max possible number of waiting cars in path
a	121	0.56	12
b	224	0.96	22
c	63	2.66	6
c*	223	2.66	22
gallery	160	0	16
d	103	2.95	10
e	423	1.10	42

4.4 Avalanche hazard

Assuming that the avalanche events are mutually exclusive and that the averaged time, t_{ei}, of exposure in the respective path i is

$$t_{ei} = \frac{(L_i + B_d)}{v}, \tag{4.1}$$

where L_i is the average length of road covered by avalanche i, B_d the stopping distance and v is the speed of the vehicle.

The avalanche hazard for total regarded stretch of road is

$$H = \frac{1}{(365)(24)(3600)} \sum_{i=1}^{N_a} (t_{ei}\ f_{ai}) \approx 2.9 \times 10^{-6} \text{ per year} \qquad (4.2)$$

Table 4.3 presents the contributions of the five paths a to e. The avalanche hazard without the present gallery is $H^* = 3.7 \times 10^{-6}$ per year. The single contributions for this case are also shown in the table.

Table 4.3 Avalanche hazard per year (R15/Grasdalen)

"Path"	a	b	c	d	e
H_i (10^{-7})	1.7	4.7	5.0	7.7	9.6
H_i^* (10^{-7})	1.7	4.7	13.0	7.7	9.6

4.5 Vulnerability

In the following no distinction between avalanche types are made and the fatality probability in a car or bus in the case of an avalanche is assumed to be

$$\lambda = 0.36, \qquad (4.3)$$

which corresponds to the mean value of the values given by (Hendrikx and Owens; 2007) for the different avalanche types (Table 2.9).

4.6 Risk

To calculate the risk, the (Hendrikx and Owens; 2007) was adapted to the conditions at several locations.

4.6.1 Moving traffic

4.6.1.1 Collective risk for moving traffic

Disregarding waiting time after an avalanche event, the collective risk with respect to car traffic is given by

$$CR_c = \beta\, \lambda \sum_{i=1}^{N_a} \left(\frac{ADT}{(24)(3600)} \frac{(L_i + B_d)}{v} f_{ai} \right) \approx 0.48 \text{ fatalities per year.} \qquad (4.4)$$

The values for ADT, λ, and β are given in Table 4.1. The collective risk with respect to bus traffic is

$$CR_b = \beta\,\lambda \sum_{i=1}^{N_a}\left(\frac{ADT}{(24)(3600)}\frac{(L_i + B_d)}{v} f_{ai}\right) \approx 0.14 \text{ fatalities per year.} \qquad (4.5)$$

Total collective risk, CR, due to avalanches for moving traffic is therefore approximately 0.62 fatal accidents per year on this stretch of road.

The collective risk without the existing gallery with respect to car, CR_c, and bus, CR_b, traffic is

$$CR_c^{\,*} \approx 0.62 \text{ fatalities per year.}$$

$$CR_b^{\,*} \approx 0.17 \text{ fatalities per year.}$$

In total, the collective risk, CR*, without gallery is about 0.79 fatal accidents per year.

4.6.1.2 Individual risk

A commuter travelling twice a day (z = 2) has a fatality risk

$$IR_C = \frac{z\,\lambda}{(24)(3600)} \sum_{i=1}^{N_a}\left(\frac{(L_{ij} + B_d)}{v} f_{ai}\right) \approx 0.8\times10^{-3} \text{ / year.} \qquad (4.6)$$

For a member of a road crew passing 6 times a day (z = 6), the individual fatality risk

$$IR_R = \frac{z\,\lambda}{(24)(3600)} \times \sum_{i=1}^{N_a}\left(\frac{(L_{ij} + B_d)}{v} \times f_{ai}\right) \approx 2.4\times10^{-3} \text{ / year.} \qquad (4.7)$$

The individual risk to die in avalanche without gallery increases to

$$IR_C^{\,*} \approx 1.0\times10^{-3} \text{ / year}$$

and

$$IR_R^{\,*} \approx 2.9\times10^{-3} \text{ / year.}$$

4.6.1.3 Summary for moving traffic

Table 4.4 gives a summary of the collective and individual risk for moving traffic with and without existing gallery.

Table 4.4 Summary of traffic risk to traffic on R15/Grasdalen excluding waiting time. Given are the expected numbers of fatalities per year for the CR and the fatality probability per year in the case of IR.

Gallery	CR_c	CR_b	IR_C	IR_R
with	0.48	0.14	$0.8\cdot10^{-3}$	$2.4\cdot10^{-3}$
without	0.62	0.17	$1.0\cdot10^{-3}$	$2.9\cdot10^{-3}$

4.6.2 Waiting traffic-Simple waiting model (car traffic)

Waiting traffic can cause serious problems as it is shown in the following.

A major concern is a second avalanche occurring while the traffic is queuing for a period in on each side of front of the avalanche deposit, while the road is plowed.

Figure 4.3 Waiting traffic in avalanche prone terrain.

In the example, there will be on average 33 cars waiting in each direction after two hours when the assumed secondary avalanche takes place.

$$NW = \frac{2}{(2)(24)} ADT \approx 33 . \tag{4.8}$$

NW is the number of waiting cars. Here, it is assumed that the amount of cars, ADT, per day and direction is uniformly distributed. No rush hour traffic is considered.

Table 4.5 provides an overview of the expected number of cars in adjacent paths after two hours. The collective risk for waiting car traffic, $CR_{w,}$ can be approximated with

$$CR_w = \sum_{i=1}^{Na} \lambda \, \beta \, P_s \sum_{k=1}^{N_k} \left(NW_{ik} \, f_{ak} \right) \approx 22.8 \text{ fatalities per year.} \tag{4.9}$$

where P_s is the probability that a secondary avalanche will run along an adjacent path k while the traffic is waiting (following Hendrikx and Owens (2007) here taken as $P_s = 0.15$).

Table 4.6 presents an overview of the contribution to CR_{wi} given the specific path i (a to e) has avalanched. However, in this case, the collective risk for waiting traffic is overestimated as one expects avalanche to occur at the end of the waiting period and thus the number of cars is overestimated.

Table 4.5 Expected numbers of waiting car, NW_{ik}, in adjacent avalanche paths after a waiting time of 2 hours assuming the cars in the gallery as being safe.

Path / Path that avalanched	a	b	c	d	e
a	0	22	6	0	0
b	12	0	6	0	0
c	11	22	0	10	7
d	0	11	6	0	33
e	0	1	6	10	0

Table 4.6 Weighted total expected numbers of affected cars in adjacent avalanche paths for a waiting time of 2 hours in a year and contribution of each individual path to the collective risk.

Path	a	b	c	d	e
$P_s \sum_{k=1}^{Nc} NW_{ik} \times f_{ak}$ (per year)	5.55	7.95	9.6	9.45	6.9
CR_{wi} (fatalities per year)	3.2	4.6	5.6	5.4	4.0

4.6.3 Modified waiting model (car traffic)

A more realistic approach assumes the second avalanche to occur any time within the waiting period. In this case, on average there will be about 17 cars waiting in each direction. Table 4.7 provides an overview of the expected number of cars, NWT_{ik}, in adjacent path within a two hours period.

Again, the modified collective risk, CR_{wm}, for the waiting car traffic might be approximated by

$$CR_{wm} = \sum_{i=1}^{Na} P_s \lambda \beta \sum_{k=1}^{N_k} (NW_{ik} f_{ak}) \approx 9.43 \text{ fatalities per year.} \quad (4.10)$$

Table 4.8 gives an overview of the contribution to CR_{wm} given a specific path has avalanched.

Table 4.7 Expected numbers of waiting car, NW_{ik}, in adjacent avalanche paths for a waiting time of 2 hours.

Path / Path that avalanched	a	b	c	d	e
a	0	17	0	0	0
b	12	0	6	0	0
c	0	17	0	1	0
d	0	0	1	0	17
e	0	0	0	10	0

Table 4.8 Weighted total expected numbers of effected cars in adjacent avalanche paths for a waiting time of 2 hours. Contribution of individual paths to the collective risk.

Path	a	b	c	d	e
$P_s \sum_{k=1}^{Nc} NW_{ik} \times f_{ak}$ (per year)	2.4	3.45	2.85	3.15	4.5
CR_{wmi} (fatalities per year)	1.4	2.0	1.7	1.9	2.6

In the case that there is no gallery, the collective risk, CR_{wm}^*, for waiting cars increases to

$$CR_{wm}^* \approx 26.19 \text{ fatalities per year.} \tag{4.11}$$

Table 4.9 shows the expected averaged number of waiting cars in the neighbouring avalanche paths and Table 4.10 depicts the individual contribution of each path to the collective risk.

Table 4.9 Expected numbers of waiting car, NWT_{ik}, in adjacent avalanche paths for a waiting time of 2 hours in the case of no gallery.

Path / Path that avalanched	a	b	c	d	e
a	0	17	0	0	0
b	12	0	17	0	0
c	0	17	0	10	70
d	0	0	17	0	17
e	0	0	7	10	0

Table 4.10 Weighted total expected numbers of affected cars in adjacent avalanches paths for a waiting time of 2 hours in the case of no gallery. Contribution of individual paths to the collective risk.

Path that avalanched	a	b	c	d	e
$P_s \sum_{k=1}^{Nc} NW_{ik}^{*} \times f_{ak}$ (per year)	2.45	7.79	18.42	9.59	7.22
CR_{wmi}^{*} (fatalities per year)	1.4	4.5	10.6	5.2	4.2

4.6.4 Waiting model (bus traffic)

The collective risk due to waiting busses may be estimated be

$$CR_{Wb} = \sum_{i=1}^{Na} P_s \, \lambda \, \beta \, NB \;\; fW_i \approx 6.83 \text{ fatalities per year} \qquad (4.12)$$

where NB is the expected number of busses in time period (NB = (2)(12)/(24) = 1). The weighted avalanche frequency, fW_i, may be written as

$$fW_i = \frac{\sum_{k=1}^{N_k} f_{ak} \; L_k \; NW_{ik}}{\left(\sum_{k=1}^{N_k} L_k \; NW_{ik} \right) + L_{gallery}} \text{ per year.} \qquad (4.13)$$

Here, $\sum_{k=1}^{N_k} L_k \; NW_{ik}$ is the length the affected roads stretch weighted with the number of cars occupying the individual stretches. Thus, the weighted frequency is a measure of a combined avalanche frequency affecting waiting bus traffic. (It is not the frequency of the single avalanche paths)

Table 4.11 Collective risk for bus traffic with a waiting time of 2 hours.

Path that avalanched	a	b	c	d	e
fW_i (per year)	0.56	0.68	1.07	0.98	1.16
CR_{Wb} (fatalities per year)	0.9	1.1	1.6	1.5	1.8

Disregarding the existing gallery, the collective risk for a waiting bus may be estimated as

$$CR_{Wb}^{*} \approx 15.77 \text{ fatalities per year} \qquad (4.14)$$

The contribution of each path is given in Table 4.12.

Table 4.12 Collective risk for bus traffic with a waiting time of 2 hours and disregarding the existing gallery

Path that avalanched	a	b	c	d	e
fW_i^* (per year)	0.96	1.92	1.31	1.63	2.75
CR_{Wb}^* (fatalities per year)	1.76	3.53	2.41	3.01	5.06

4.6.5 Individual risk due to waiting for a commuter

The individual risk for a commuter (z=2) of being killed while waiting may be approximated by

$$IR_w = z\,\lambda\,P_S\,\frac{2}{24}\sum_{i=1}^{Na} fW_i \approx 0.04 \text{ fatality probability per year.} \quad (4.15)$$

Without gallery, the individual risk for a waiting commuter increase to

$$IR_w^* \approx 0.08 \text{ fatality probability per year.} \quad (4.16)$$

4.6.6 Summary

The stretch of RV15 at Grasdalen represents a major risk to the traffic. Table 4.13 summarizes the collective risk calculated with and without a protection gallery. The total collective risk, CR_{tot2}, accounts for that a waiting bus replaces approximately 2 cars.

It can be seen that the waiting traffic is a major problem as collective risk increases significantly. This was also quoted by Hendrikx and Owens (2007). The calculations suggest high collective risk with 15.7 and 32.7 expected fatalities per year, which is far beyond the observed one. However, in this calculation, it was assumed that no special mitigation measures where taken in the case of an avalanche event, like road closure and enforcing of cars to wait in safe spots, which will usually be the case. In addition, it was assumed in the calculations that an avalanche event takes the full width of the path, which is also an overestimate.

The table also illustrates the benefit of the gallery, which approximately halves the collective risk. However, this reduction is most effective for the waiting traffic, a situation, which should be avoided in any case.

Table 4.13 Summary of collective risk with and without present gallery (fatalities per year).

Collective risk	CR_c	CR_b	CR_{wc}	CR_{wb}	CR_{tot}	CR_{tot2}
with gallery	0.5	0.1	9.4	6.8	16.9	15.7
without gallery	0.6	0.2	26.2	15.8	33.8	32.7

Subscripts mark: c = car; b = bus; wc = waiting car; wb = waiting bus; total risk; tot2 = total risk accounting for replaces car by busses.

The individual risk of a commuter and for members of a road crew is summarized in Table 4.14. Here again, one sees the influence of waiting time and protection gallery.

Table 4.14 Summary of individual risk with and without existing gallery for a commuter IR_C travelling twice a day and for a member of a road crew, IR_R, passing 6 times a day (fatality probability per year). The individual risk for a member of a crew does not include the additional risk during elongated exposure time during avalanche clearing work.

Individual risk (fatality probability per year)	Commuter IR_C	Commuter waiting IR_{wC}	Commuter total IR_{Ctot}	Road crew IR_R
with gallery	$0.8 \cdot 10^{-3}$	$40 \cdot 10^{-3}$	$40.8 \cdot 10^{-3}$	$2.4 \cdot 10^{-3}$
without gallery	$1.0 \cdot 10^{-3}$	$80 \cdot 10^{-3}$	$81.0 \cdot 10^{-3}$	$2.9 \cdot 10^{-3}$

5 REFERENCES

Bakkehoi, S., Domaas, U. & Lied, K. (1983). Calculation of snow avalanche runout distance, *Annals of Glaciology, 4*, 24-29

Bakkehoi, S. (1987). Snow avalanche prediction using a probabilistic method. In Salm, B. & Gubler, H. (ed.) Avalanche Formation, Movements and Effects. Proceedings of the Davos Symposium, September 1986, IAHS Press, 162, 549-555

Barbolini, M. & Savi, F. (2001). Estimate of uncertainties in avalanche hazard mapping, Annals of Glaciology, 32, 299-305

Düzgün, H.S.B. & Lacasse, S. (2005). Vulnerability and acceptable risk in integrated risk assessment framework. In O. Hungr and R. Fell and R. Couture and E. Eberhardt (Editor) Landslide Risk Management, 505-515.

Frutiger, H. (1980). History and actual state of legalization of avalanche zoning in Switzerland *Journal of Glaciology, 26*, 313-324

Harbitz, C., Harbitz, A. & Nadim, F. (2001). On probability analysis in snow avalanche hazard zoning *Annals of Glaciology, 32*, 290-298

Hendrikx, J. & Owens, I. (2007). Modified avalanche risk equations to account for waiting traffic on avalanche prone roads *Cold Regions Science and Technology,* **2007**, *51*, 214-218

Hendrikx, J., Owens, I., Carran, W. & Carran, A. (2006). Avalanche risk evaluation with practical suggestions for risk minimization: A case study of the

Milford road, New Zealand *Proceedings of the International Snow Science Workshop 2006, Telluride, Colorado, United States, pp.* 757-767

Keylock, C.J., McClung, D.M. & Magnusson, M.M. (1999). Avalanche risk mapping by simulation *Journal of Glaciology,* **1999**, *45*, 303-314

Keylock, C.J. & Barbolini, M. (2001). Snow avalanche impact pressure – vulnerability relations for use in risk assessment *Canadian Geotechnical Journal, 38*, 227-238

Keylock, C.J. (2005). An alternative form for the statistical distribution of extreme avalanche runout distances *Cold Regions Science and Technology, 42*, 185-193

Körner, H.J. (1980). The energy-line method in the mechanics of avalanches *Journal of Glaciology, 26*, 501-505

Kristensen, K., Harbitz, C.B. & Harbitz, A. (2003). Road traffic and avalanches - Methods for risk evaluation and risk management *Surveys in Geophysics, 24*, 603-616

Kristensen, K., Harbitz, C. & Harbitz, A. (2003). The EU program CADZIE: Road traffic and avalanches -- methods for risk evaluation and risk management *Norwegian Geotechnical Institute. NGI report 20001289-4*

Margreth, S., Stoffel, L. & Wilhelm, C. (2003). Winter opening of high alpine pass roads--analysis and case studies from the Swiss Alps, *Cold Regions Science and Technology, 37*, 467-482

McClung, D.M. (2005). Risk-based definition of zones for land-use planning in snow avalanche terrain *Canadian Geotechnical Journal, 42*, 1030-1038

McClung, D.M. (2001). Extreme avalanche runout: A comparison of empirical models *Canadian Geotechnical Journal, 38*, 1254-1265

McClung, D.M. (2000). Extreme avalanche runout in space and time, *Canadian Geotechnical Journal, 37*, 161-170

McClung, D.M. (1999). The encounter probability for mountain slope hazards, *Canadian Geotechnical Journal, 36*, 1195-1196

McClung, D.M. & Schaerer, P. The Avalanche Handbook The Mountaineers, 3-Edition, 2006

Norem, H., Irgens, F. & Schieldrop, B. (1987). A continuum model for calculating snow avalanche velocities. In Salm, B. & Gubler, H. (ed.) Avalanche

Formation, Movements and Effects. Proceedings of the Davos Symposium, September 1986, IAHS Press, 162, 363--380

Perla, R., Cheng, T. T. & McClung, D.M. (1980). A Two-Parameter Model of Snow-Avalanche Motion Journal of Glaciology, 26, 119-207

Schaerer, P. (1989). The avalanche-hazard index *Annals of Glaciology, 13*, 241-247

Valentine, G.A. (1998). Damage to structures by pyroclastic flows and surges, inferred from nuclear weapons effects *Journal of Volcanology and Geothermal Research, 87*, 117-140

Wilhelm, C. (1997). Wirtschaftlichkeit im Lawinenschutz: Methodik und Erhebungen zur Beurteilung von Schutzmassnahmen mittels quantitativer Risikoanalyse und ökonomischer Bewertung, *Eidgenöss. Inst. Schnee- Lawinenforsch., Davos,* 146

6 APPENDIX

6.1 Canadian Snow Avalanche Size Classification System and typical Factors (McClung and Schaerer, 2006)

Table 6-1 Canadian Snow Avalanche Size Classification System and typical Factors (McClung and Schaerer, 2006)

Size	Description	Typical mass (Mg)	Typical path length (m)	Typical impact pressure (kPa)
1	Relative harmless to people	$< 10^1$	10	1
2	Could bury, injure or kill a person	10^2	100	10
3	Could bury a car, destroy a small building, or break a few trees	10^3	1000	100
4	Could destroy a railway car, large truck, several buildings, or a forest with an area up to 4 hectares	10^4	2000	500
5	Largest snow avalanche known; could destroy a village or a forest of 40 hectares	10^5	3000	1000

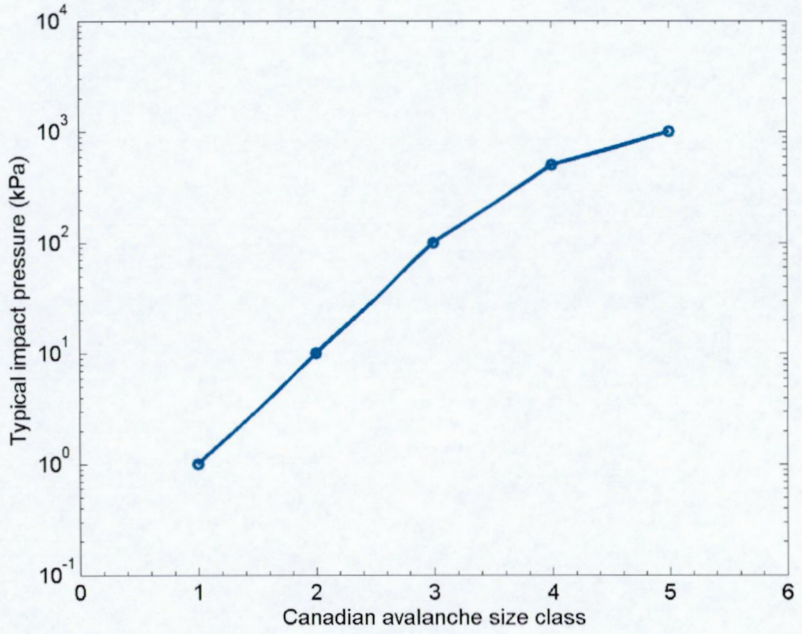

Figure 6.1 Typical impact pressures corresponding to the Canadian Avalanche Size Classification after (McClung and Schaerer, 2007)